Journal of Cleaner Production 415 (2023) 137792

Contents lists available at ScienceDirect

Journal of Cleaner Production

journal homepage: www.elsevier.com/locate/jclepro

Greywater treatment for reuse: Effect of combined foam fractionation and persulfate-iron based fenton process in the bacterial removal and degradation of organic matter and surfactants

Antonio Faggiano [a], Maria Ricciardi [a], Oriana Motta [b], Antonino Fiorentino [a,*], Antonio Proto [a]

[a] Department of Chemistry and Biology "Adolfo Zambelli", University of Salerno, Via Giovanni Paolo II 132, 84084, Fisciano, SA, Italy
[b] Department of Medicine Surgery and Dentistry "Scuola Medica Salernitana", University of Salerno, Via S. Allende 1, 84081, Baronissi, SA, Italy

ARTICLE INFO

Handling Editor: Jin-Kuk Kim

Keywords:
Disinfection
Anionic surfactants
Advanced oxidation process
Wastewater reuse
P. aeruginosa
E. coli

ABSTRACT

Greywater (GW) represents a viable candidate in adapting to increased water scarcity due to climate change because its reuse can significantly reduce domestic water consumption. This work focused on studying the combination of physical foam fractionation (FF) as pre-treatment step and Fenton processes as polishing-step. The FF, applied for first time on real GW, allowed reaching a removal of 60 and 85% for chemical oxygen demand (COD) and total surfactants (TSU), respectively, and a bacterial removal of about 3Log units. Fenton processes using $Fe^{2+}/S_2O_8^{2-}$ and Fe^{2+}/H_2O_2 were optimized through response surface methodology (RSM) with a central composite design (CCD). The concentration of Fe^{2+}, oxidant and treatment time were chosen as variable factors, while COD and TSU removals as target responses. According to RSM results, the optimum conditions to operate Fenton processes were (mg/L) Fe^{2+}:12.5/$S_2O_8^{2-}$:185.6 and Fe^{2+}:50/H_2O_2:157.6 with a treatment time of 30 min for both processes. A COD removal of 89 and 78% and TSU removals of 99.7 and 96.6% were obtained for $Fe^{2+}/S_2O_8^{2-}$ and Fe^{2+}/H_2O_2 respectively. Complete bacterial removal was detected for both Fenton processes. $Fe^{2+}/S_2O_8^{2-}$ allowed for a 4-fold lower sludge production than Fe^{2+}/H_2O_2. The persulfate-based process requires low treatment time (2.5 h) and energy consumption with limited sludge production, making it a promising technology for future research and full-scale application.

1. Introduction

Water scarcity and the increasing demand for fresh water due to a growing population are two major global problems that have been steadily increasing (Gómez-Monsalve et al., 2022; Kummu et al., 2016; Mekonnen and Hoekstra, 2016). These challenges have led to research focusing on the development of new technologies to treat wastewater for reuse in agriculture, aquaculture, groundwater recharge and other sectors (Soriano-Molina et al., 2021). In this context, greywater (GW) is an excellent candidate on the one hand because it accounts for about 50–80% of domestic wastewater (DWW) and on the other hand because it appears to have lower organic and pathogenic microorganism load than municipal wastewater (Filali et al., 2022; Khosravanipour Mostafazadeh et al., 2019; Pidou et al., 2007; Schoen et al., 2021; Silva et al., 2023). GW is defined as DWW derived from the shower, washing machine, kitchen sink, dishwasher and washbasin (Boyjoo et al., 2013; Khanam and Patidar, 2022). GW can be further classified into light (LGW) from showers and washbasin, and dark (DGW) from laundry and kitchen sources, which typically contains higher concentrations of organic matter (Albalawneh and Chang, 2015). The quality of GW depends enormously on the source and the habits of the houses in which it is produced (Spychała et al., 2019). Soap accounts for approximately 90% of mass loading in a hand basin (Maimon et al., 2010; Ziemba et al., 2018), while bathroom greywater consist mainly of constituents such as shampoo, soap, toothpaste, hairs, skin, body fats and body care products (Kadewa et al., 2020; Noah, 2002). An analysis of recent reviews emerges reveals that the DGW and LGW are different in chemical composition depending on the source and the country of production (low-income or high-income countries) (Ghaitidak and Yadav, 2013; Shaikh and Ahammed, 2020). As a result, estimating mean values of the main chemical parameters in GW becomes challenging. Nevertheless, LGW have been found to contain values up to 1488, 673, 148 and 60 mg/L for COD, 5-days biochemical oxygen demand (BOD_5), total nitrogen (TN) and total phosphorus (TP) respectively, while DGW has exhibited values up to 8071, 3330, 65 and 187 mg/L for the same

* Corresponding author.
E-mail address: afiorentino@unisa.it (A. Fiorentino).

https://doi.org/10.1016/j.jclepro.2023.137792
Received 16 March 2023; Received in revised form 9 June 2023; Accepted 11 June 2023
Available online 17 June 2023

Abbreviations

AOPs	advanced oxidation processes
ASU	anionic surfactants
BOD_5	biochemical oxygen demand
BPB	bromophenol blue
CCA	Chromogenic Coliforms Agar
COD	chemical oxygen demand
CSU	cationic surfactants
CTAB	cetyltrimethylammonium bromide,
DGW	dark greywater
DWW	domestic wastewater
E. coli	Escherichia *E. coli*
FF	foam fractionation
GW	greywater
LGW	light greywater
NISU	non-ionic surfactants
P. aeruginosa	Pseudomonas aeruginosa
RSM	response surface methodology
SDS	sodium dodecyl sulphate
TBPEE	tetrabromophenolphthalein ethyl ester
TC	total coliforms
TN	total nitrogen
TP	total phosphorus
TSU	total surfactants
TRX-100	triton X-100
WWTPs	Wastewater treatment plants

Table 1
Main LGW and DGW characteristics from literature review.

Parameter	LGW	DGW
COD (mg/L)	23–1489	58–8071
BOD_5 (mg/L)	20–673	44–3330
TN (mg/L)	1.3–148	0.5–65
TP (mg/L)	0.1–60	0.2–187
E. coli (CFU/100 mL)	1×10^6	4×10^6
TC (CFU/100 mL)	1×10^9	7×10^7
P. aeruginosa (CFU/100 mL)	3×10^3	5×10^3

parameters. While values up to 1×10^9, 1×10^6 and 3×10^3 CFU/100 mL in LGW and 7×10^7, 4×10^6 and 5×10^3 CFU/100 mL in DGW have been detected for *Total coliforms* (*TC*), *Escherichia coli* (*E. coli*) and *Pseudomonas aeruginosa* (*P. aeruginosa*) respectively (Blanky et al., 2015; Shaikh and Ahammed, 2020). Main LGW and DGW characteristics are showed in Table 1.

P. aeruginosa is considered an alternative indicator to *E. coli* for assessing the microbiological quality of GW, due to their superior ability to reproduce and persist in waters characterised by low nutrient availability (Teodoro et al., 2018). The main components of GW are soaps and detergents, which act as foaming agents. These water matrices typically contain significant concentrations of anionic surfactants (ASU), such as sodium dodecyl sulphate (SDS), with levels reaching up to 118 mg/L. Minor concentrations of non-ionic surfactants (NISU), such as polyethoxylated surfactants, and cationic surfactants (CSU), such as Benzalkonium chloride, are also commonly detected(Ghaitidak and Yadav, 2013) are usually detected in these water matrices. Surfactants are classified as emerging contaminants and pose a major challenge in wastewater treatment. They are difficult to remove and have numerous potential negative impacts on the environment due to their high level of toxicity (Lechuga et al., 2016; Palmer and Hatley, 2018). Furthermore, studies indicate that the presence of surfactants in wastewater intended for reuse in irrigation can be harmful to crops, as they contribute to the absorption of hydrocarbons by the soil (Hardie et al., 2021; Ying, 2006). GWs represent an excellent opportunity for wastewater reuse in worldwide, aligning with the goals of the Agenda 2030 ("Agenda 2030," n.d.). However, reuse regulations sometimes represent a major obstacle, as they are very stringent in several countries. The most commonly required minimum regulatory limits include 100 mg/L, 20 mg/L for BOD_5 and 10 CFU/100 mL for *TC* and *E. coli*, (Shoushtarian and Negahban-Azar, 2020). Additionally, specific regulatory limits of 0.5 mg/L for total surfactants (TSU) in Italy and 0.2 mg/L for anionic surfactants (ASU) in Australia have been imposed (Shoushtarian and Negahban-Azar, 2020). To achieve the appropriate quality for GW reuse, a combination of different treatment processes, typically involving physical and chemical methods, along with a final disinfection step, is required (Elmitwalli and Otterpohl, 2007; Filali et al., 2022; F. F. Li et al., 2009; Šostar-Turk et al., 2005). In recent years, advanced oxidation processes (AOPs) have been investigated as pre- or post-treatment for GWs. These processes facilitate the in-situ generation of powerful oxidising agents, such as hydroxyl radicals (•OH), which can effectively oxidize and mineralize organic matter (de Simone Souza et al., 2023; Faggiano et al., 2023; Pesqueira et al., 2021), including chemical compounds like surfactants, while simultaneously removing bacteria (Fiorentino et al., 2017, 2022). Among AOPs, H_2O_2/Fe^{2+} (Wagdy et al., 2022), UV/H_2O_2 (Chin et al., 2009; Cibati et al., 2022) and $UV/TiO2/H_2O_2/Fe$ (Tsoumachidou et al., 2017) have shown good performance in terms of COD and BOD_5 removal. The most investigated oxidant agent in AOPs is H_2O_2 but in recent years, persulfate anion ($S_2O_8^{2-}$) has also been studied for wastewater treatment and the removal of contaminants of emerging concerns. $S_2O_8^{2-}$ offers several advantages over H_2O_2. SO_4[] radicals have a higher reduction potential (2.5–3.1 V) compared to •OH radicals (1.8–2.7 V), resulting in a greater selectivity for oxidation reactions. Additionally, $S_2O_8^{2-}$ has a longer half-life period ($t_{1/2}$ = 30–40 μs) compared to H_2O_2 (20 ns) (Arellano et al., 2019; Ghanbari and Moradi, 2017). In a recent study, researchers investigated the combination of an economical and easy-to-operate physical process by a system of foam fractionation (FF) followed by sunlight/H_2O_2/-Fe-IDS for the removal of COD and BOD_5 in synthetic LGW. Promising results were obtained with COD and BOD_5 removal efficiencies of 89.5% and 75.8% respectively (Faggiano et al., 2022). To the best of the authors' knowledge, FF has not been previously studied in the removal of surfactants removal or disinfection of GW. Furthermore, the use of $Fe^{2+}/S_2O_8^{2-}$ has not been investigated in GW treatment. This study aimed to investigate, for the first time, the removal of COD, BOD $_5$, TN, TP, ASU, NISU and bacteria (*E. coli, P. aeruginosa* and *TC*) using FF as the main treatment method for real LGW. Additionally, post-treatment using two different Fenton processes (Fe^{2+}/H_2O_2 and $Fe^{2+}/S_2O_8^{2-}$) was investigated and optimized by RSM approach to achieve LGW quality suitable for the reuse. Specifically, a two-level factorial design coupled with RSM was selected for the experimental design. The operating conditions were optimized in terms of H_2O_2, $S_2O_8^{2-}$, Fe^{2+} doses and treatment time to achieve the desired removal of COD, ASU and NISU (target responses).

2. Materials and methods

2.1. GW samples

Synthetic LGW were prepared following the guidelines provided by the Australian Commonwealth Scientific and Industrial Research organization, as done in previous studied, considering 4 as the number of members per household and adjusting the doses based on typical habits (Faggiano et al., 2022). A combination of various detergents used for

Table 2
Average characteristics of synthetic and real LGW.

Parameter	Synthetic LGW	Real LGW
pH	8.2 ± 0.1	7.9 ± 0.1
EC[a] (mS/cm)	650 ± 25	610 ± 15
COD (mg/L)	650 ± 35	600 ± 88
BOD_5 (mg/L)	100 ± 20	85 ± 15
ASU (mg/L)	50.3 ± 0.4	43.4 ± 0.3
NISU (mg/L)	8.1 ± 0.6	5.7 ± 0.2
CSU (mg/L)	0.3 ± 0.1	ND
TSU (mg/L)	58.7 ± 1.1	49.1 ± 0.5
TN (mg/L)	24 ± 3	16 ± 4
TP (mg/L)	13 ± 4	7 ± 2
TC (CFU/100 mL)	ND	$2.7 \times 10^4 \pm 4.1 \times 10^3$
E. coli (CFU/100 mL)	ND	$3.3 \times 10^3 \pm 1.1 \times 10^3$
P. aeruginosa (CFU/100 mL)	ND	$2.5 \times 10^4 \pm 2.3 \times 10^3$

[a] EC: electrical conductivity.

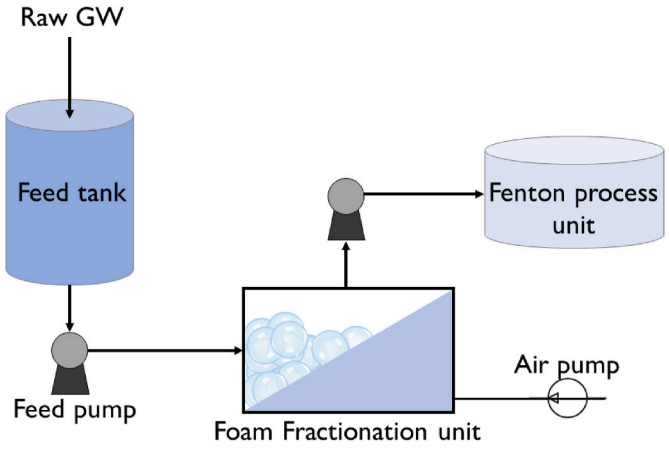

Fig. 1. Treatment process flow for LGW treatment.

personal hygiene and household cleaning, including toothpaste, shampoo, hand soap, shower gel and chlorine beach, was used to obtain the synthetic LGW. Real LGW samples used in this study were collected from several buildings located in Salerno (Italy), throughout different period of the year. The samples were collected from bathrooms with sink and shower discharges. 2 L of real GW was manually collected in polyethene bottles from 10 different utilities. Subsequently, 1 L from each bottle was combined to obtain a composite sample of 10 L in a polyethene container. The composite sample was then transported directly from the building directly to the laboratory and used in the experiments on the same day as collection. The composition of LGW can vary depending on the activities of the building inhabitants. Table 2 provides a summary of the average characteristics of the synthetic and real LGW used in this study during the experimental stages.

Real LGW samples with COD values superior of 700 mg/L or lower than 500 mg/L were excluded from the experiments. Out of 15 samples collected, 3 samples were removed from the analysis as they were considered outliers. Specifically, the characteristics of one sample was suitable, in terms of COD, BOD_5 and TSU for its reuse. However, two samples exhibited significantly higher COD and BOD_5 values compared to the others (1280 mg/L and 360 mg/L respectively), and thus, they were excluded as they were the only two outliers with such a high organic load.

2.2. Chemicals

Iron(II) sulphate heptaydrate ($FeSO_4 \bullet 7H_2O$), hydrogen peroxide (H_2O_2) 30% wt, potassium hydrogen phthalate ($C_8H_5KO_4$), potassium dichromate ($K_2Cr_2O_7$), silver sulphate (Ag_2SO_4), mercury sulphate ($HgSO_4$), potassium persulfate ($K_2S_2O_8$) and sulfuric acid (H_2SO_4) 98%, Tetrabromophenolphthalein ethyl ester (TBPEE), bromophenol blue (BPB), methylene blue, sodium tetraborate ($Na_2B_4O_7$), chloroform, dichloromethane, ethanol (EtOH) and tert-butyl alcohol (TBA) were purchased from Sigma Aldrich (Saint Louis, MO, USA), and used without further purification. Chromogenic Coliforms Agar (CCA) and Pseudomonas CN Agar were purchased from Condalab.

2.3. Experimental set-up of FF

The process flow (Fig. 1) involved a feed tank for LGW, from which the samples were transferred to the FF unit using a peristaltic pump. The FF unit operated in batch mode and consisted of two Pyrex glass bottles (diameter: 13 cm, height: 30 cm) with a volume of 1 L each, connected serially. The first bottle, once filled with 1 L of sample, was hermetically sealed and aerated to promote foam formation. The aeration was achieved by suppling air through a Pyrex gas washing bottle with a Drechsel head form (DURAN®), positioned 30 cm from the bottom of the bottle. The foam generated in the first bottle then flowed into the second bottle through a connecting pipe and could be removed. The air flow rate was set to 3 L/min based on previous results (Faggiano et al., 2022).

2.4. Experimental set-up of fenton processes

The Fenton tests were conducted in batch mode. A 1 L beaker was filled with 500 mL of pre-treated GW transferred from the FF unit using a peristaltic pump. The temperature was maintained at a constant level of 25 ± 1 °C using a thermostatic probe. Temperature, pH, EC, BOD_5, COD, TN, TP, ASU, NISU, residual H_2O_2 concentrations and residual $S_2O_8^{2-}$ concentration were monitored during the tests. Reagents were added in the following order: the sulfuric acid was added and stirred until pH value reached 2.8, then $FeSO_4 \cdot 7H_2O$ solution was added and stirred for about 1 min before adding the oxidant. After the addition of oxidant, the process time started. The kinetic studies in the optimized process were conducted in triplicate. Following the Fenton oxidation process, precipitation of Fe^{2+} as hydroxides and the coagulation process were performed using a jar test apparatus. This process consisted of four steps: (i) pH adjustment to 8 with NaOH; (ii) fast mixing (at 150 rpm) of GW for 2 min; (iii), slow mixing (at 35 rpm) for 30 min to induce the flocs' formation; and, (iv), 1 h of sludge sedimentation without agitation at 150 rpm for 2 min and 35 rpm for 30 min prior to analytical determinations.

2.5. Analytical measurement

2.5.1. Main chemical parameters

BOD_5 was measured by manometric respiration tests according to OECD301F with the OxiTop® Control measuring system. Samples containing H_2O_2 were violently stirred for several hours until complete degradation of H_2O_2 in accordance with the APHA 5210 Biochemical Oxygen Demand (BOD) method (APHA, 1998). COD was measured using the spectrophotometric method proposed by Li et al. (J. J. Li et al., 2009). A spectrometer (HR 2000, Ocean Optics, USA) equipped with a CC-3-UV-S cosine corrector with Spectralon as diffusing material was used to measure the irradiance spectra of the UV lamp. Residual $S_2O_8^{2-}$ was measured spectrophotometrically using a reported method based on modification of the iodometric titration method (Liang et al., 2008). Briefly the analysis of absorption spectra of a yellow colour solution resulting from the reaction of persulfate and iodide in the presence of sodium bicarbonate reveals an absorbance at 352 nm, without significant interferences from the reagent matrix. Calibration curve was liner between 0 and 1 g/L. Residual H_2O_2 concentration was analyzed by a spectrophotometric method based on the use of titanium(IV) oxysulfate, which forms a stable yellow complex with H_2O_2 detected at a wavelength of 410 nm (Fiorentino et al., 2019). The absorbance measurement was linearly correlated with standard H_2O_2 concentration in the range of 0.1–100 mg/L (Fiorentino et al., 2015). To account for the interference of H_2O_2 on COD measurement, the correlation between H_2O_2 and COD

Table 3
Ranges and levels for each factor.

Variables	Code	Range and levels			
		L1	L2	L3	L4
Fe^{2+} (mg/L)	X_1	12.5	25	37.5	50
Oxidant concentration (mg/L)	X_2	65.5	131	196.5	262
Time (min.)	X_3	15	20	45	60
Oxidant type	X_4	–	H_2O_2	$S_2O_8^{2-}$	–

was calculated as follows (Talinli and Anderson, 1992):

$$COD = COD_m - d{\cdot}f \quad \text{Eq. 1}$$

Where:

COD_m is measured COD (mg/L)

d is H_2O_2 concentration in the sample (mg/L)

f is correction factor = 0.25. It is valid for 20–1000 mg/L H_2O_2.

For the interference of $S_2O_8^{2-}$ in COD measurement, a correlation curve was obtained measuring COD of standard $S_2O_8^{2-}$ solutions (Zhang et al., 2014). A linear relationship was observed between 0 and 300 mg/L (the range of $S_2O_8^{2-}$ used in the present study was 65.5–262 mg/L) with a determination coefficient (R^2) of 0.998. The COD values were calculated as follows:

$$COD = COD_m - COD_{PS}$$

Where:

COD_m is measured COD (mg/L)

COD_{PS} the influence of $S_2O_8^{2-}$ concentration obtained from the calibration curve

TN, TP, dissolved Fe, were analyzed follow "Standard Methods for the Examination of Water and Wastewater" 4500-N C, 4500-P, and 3500-Fe respectively (APHA, 1998). Sludge production (volume) was estimated through standard method for settleable solids (APHA 2540 f) (APHA, 1998) by taking 1L of homogenized effluent after the treatment and allowed to settle down in a 1 L graduated Imhoff cone for 45 min. After the settlement the sludge volume was recorded as mL of sludge for L of treated wastewater.

2.5.2. Surfactants determination

ASU were measured using an adapted version of the methylene blue active substance (MBAS) procedure outlined in APHA 5540-C (APHA, 1998; Jurado et al., 2006). First, 0.2 mL of $Na_2B_4O_7$ buffer solution (19.07 g/L), followed by 0.32 mL of methylene blue solution (250 mg/L) were added to 5 mL of sample. ASU react in alkaline medium with methylene blue to form a stable complex which is extracted from the sample with 3 mL of chloroform. The chloroform phase was analyzed spectrophotometrically at a wavelength of 650 nm. The calibration curve was obtained following the same procedure for standard solution of SDS in the range 0.0–3.5 mg/L. NISU were measured by an adapted TBPEE method (Tôei et al., 1982). NISU react with TBPEE to form a stable yellow complex. 3 mL of sample were added to 3 mL of TBPEE sodium salt solution in dichloromethane (20 mg/L), then a liquid-liquid extraction was performed. The dichloromethane yellow-green phase was analyzed spectrophotometrically at a wavelength of 606 nm. The calibration curve was obtained following the same procedure for standard solution of Triton X-100 (TRX-100) in the range 0.0–2.5 mg/L. CSU were measured using the BPB method (Kamaya et al., 1999; Sakai et al., 1992). 0.32 mL of BPB sodium salt solution (250 mg/L) was added to 5 mL of sample. CSU react with BPB to form a stable yellow complex which is extracted from the sample with 3 mL of chloroform. The chloroform phase was analyzed spectrophotometrically at a wavelength of 420 nm. The calibration curve was obtained following the same procedure for standard solution of cetyltrimethylammonium bromide (CTAB) in the range 0.0–2.5 mg/L. TSU was obtained from the sum of ASU, NISU and CSU.

Table 4
RSM design in coded units and the corresponding natural values.

Experiment number	Fe^{3+} (mg/L)	Oxidant concentration (mg/L)	Time (min.)	Oxidant type
1	37.50	196.5	15.00	$S_2O_8^{2-}$
2	12.50	65.50	15.00	H_2O_2
3	37.50	196.5	20.00	H_2O_2
4	37.50	196.5	20.00	H_2O_2
5	25.00	65.50	60.00	H_2O_2
6	50.00	65.50	30.00	H_2O_2
7	12.50	196.5	45.00	H_2O_2
8	50.00	65.50	15.00	$S_2O_8^{2-}$
9	25.00	65.50	30.00	$S_2O_8^{2-}$
10	50.00	131.0	45.00	$S_2O_8^{2-}$
11	25.00	131.0	45.00	$S_2O_8^{2-}$
12	25.00	262.0	45.00	$S_2O_8^{2-}$
13	25.00	262.0	30.00	$S_2O_8^{2-}$
14	50.00	262.0	30.00	$S_2O_8^{2-}$
15	25.00	65.50	60.00	H_2O_2
16	50.00	262.0	60.00	H_2O_2
17	50.00	131.0	30.00	$S_2O_8^{2-}$
18	12.50	262.0	15.00	H_2O_2
19	12.50	196.5	15.00	$S_2O_8^{2-}$
20	12.50	65.50	60.00	$S_2O_8^{2-}$
21	12.50	196.5	45.00	H_2O_2
22	37.50	196.5	45.00	$S_2O_8^{2-}$
23	25.00	65.50	30.00	$S_2O_8^{2-}$
24	37.50	196.5	20.00	H_2O_2

2.6. Identification and bacterial count

Bacterial concentration in each LGW sample was estimated using the membrane filtration method, with a serial 10-fold dilution in phosphate buffer saline (PBS). A volume of 100 mL of the sample was filtered through cellulose nitrate membranes filters (0.45 μm pore size, Merck Millipore®). The membranes were then cultivated for 24 h at 36 ± 2 °C in CCA culture medium, a selective chromogenic medium for the detection of *TC* and *E. coli* and Pseudomonas CN Agar culture medium for the detection of *P. aeruginosa.* Measurements were carried out in triplicate, and the average value and standard deviation were plotted as $\log_{10}$ (CFU/100 mL). Controls were performed to ensure the bacterial viability during the treatment time. For each experiment, a LGW sample was stored in the dark until the end of the assay (150 min) to perform bacterial counts before and after treatment. Controls with H_2O_2 and $S_2O_8^{2-}$ alone were also conducted, but no effects on bacterial removal were observed. In all cases, no decrease in CFU/100 mL was observed for the controls. At the end of FF, $Fe^{2+}/S_2O_8^{2-}$ and Fe^{2+}/H_2O_2 experiments, treated samples were incubated at 20 ± 2 °C for 24, 48 and 72 h to evaluate bacterial regrowth for all three bacteria species examined, following the procedure described in a previous work (Fiorentino et al., 2021).

2.7. Response surface design and statistical model

In this study, RSM was utilized for the experimental design of the Fenton processes. The concentration of Fe^{2+} (X1), the oxidant concentration (X2) and treatment time were chosen as numerical factors, while the type of oxidant (H_2O_2 or $S_2O_8^{2-}$) (X3) was selected as a categorical factor. Discrete values for the factors (Fe^{2+}, oxidant concentration and time) were chosen based on the results of preliminary tests, aiming to achieve residual oxidant concentrations (both for H_2O_2 and $S_2O_8^{2-}$) lower than 0.2 mg/L after 1 h of treatment. The ranges and levels for each factor, as well as the RSM design, are presented in Tables 3 and 4, respectively.

The two responses were estimated through a quadratic model according to Eq. (2):

$$Y = b_0 + \sum_{i=1}^{n} b_i X_i + \sum_{i=1}^{n} b_{ii} X_i^2 + \sum_{i=1}^{n} b_{ij} X_i X_j + \varepsilon \quad \text{Eq. 2}$$

Table 5
Reaction schemes considered for kinetic study.

Reaction	k_i (M^{-1} s^{-1})
Fe^{2+}/H_2O_2 process	
$Fe^{2+} + H_2O_2 \xrightarrow{k_1} Fe^{3+} + HO^{\cdot} + HO^-$	76[a]
$Fe^{3+} + H_2O_2 \xrightarrow{k_2} Fe^{2+} + HO_2^{\cdot} + H^+$	0.02[a]
$Fe^{2+} + HO^{\cdot} \xrightarrow{k_3} Fe^{3+} + HO^-$	4.8×10^8 [a]
$H_2O_2 + HO^{\cdot} \xrightarrow{k_4} HO_2^{\cdot} + H_2O$	7×10^7 [b]
$TSU + HO^{\cdot} \xrightarrow{k_5} P_i$	k_4[c]
$Fe^{2+}/S_2O_8^{2-}$ process	
$Fe^{2+} + S_2O_8^{2-} \xrightarrow{k_6} Fe^{3+} + SO_4^{\cdot -} + SO_4^{2-}$	15.33[a]
$S_2O_8^{2-} + SO_4^{\cdot -} \xrightarrow{k_7} S_2O_8^{\cdot -} + SO_4^{2-}$	6.62×10^5 [a]
$Fe^{2+} + SO_4^{\cdot -} \xrightarrow{k_8} Fe^{3+} + SO_4^{2-}$	4.6×10^9 [a]
$TSU + SO_4^{\cdot -} \xrightarrow{k_9} TSU_i$	k_9[c]

[a] (Kusic et al., 2011).
[b] (Giménez et al., 2023).
[c] Value calculated in this work.

Table 6
Reaction rates for the studied species.

Reaction rate expressions
Fe^{2+}/H_2O_2 process
$R_{H_2O_2} = -k_1[H_2O_2][Fe^{2+}] - k_2[Fe^{3+}][H_2O_2] - k_4[H_2O_2][HO^{\bullet}]$
$R_{Fe^{2+},H_2O_2} = -k_1[H_2O_2][Fe^{2+}] + k_2[Fe^{3+}][H_2O_2]$
$R_{Fe^{3+},H_2O_2} = -R_{Fe^{2+},H_2O_2}$
$R_{HO^{\cdot}} = k_1[H_2O_2] - k_3[Fe^{2+}][HO^{\cdot}] - k_4[H_2O_2][HO^{\cdot}] - k_5[TSU][HO^{\cdot}]$
$R_{TSU,H_2O_2} = -k_5[TSU][HO^{\cdot}]$
$Fe^{2+}/S_2O_8^{2-}$ process
$R_{S_2O_8^{2-}} = -k_6[S_2O_8^{2-}][Fe^{2+}] - k_7[S_2O_8^{2-}][SO_4^{\cdot -}]$
$R_{Fe^{2+},S_2O_8^{2-}} = -k_6[S_2O_8^{2-}][Fe^{2+}] - k_8[SO_4^{\cdot -}][Fe^{2+}]$
$R_{Fe^{3+},S_2O_8^{2-}} = -R_{Fe^{2+},S_2O_8^{2-}}$
$R_{SO_4^{\cdot -}} = k_6[Fe^{2+}][S_2O_8^{2-}] - k_7[S_2O_8^{2-}][SO_4^{\cdot -}] - k_8[Fe^{2+}][SO_4^{\cdot -}] - k_9[TSU][SO_4^{\cdot -}]$
$R_{TSU,S_2O_8^{2-}} = -k_9[TSU][SO_4^{\cdot -}]$

Y is the response of COD or TSU removal, b_0 is a constant, b_i correspond to linear coefficient of X_i, b_{ii} is the second order effect on regression coefficients, b_{ij} is the interaction coefficient and ε is the statistical error.

After the calculation of the optimal process in terms of catalyst, oxidant concentration and treatment time, three replicates of this process were made and the kinetics of both COD and TSU removal were calculated.

For the optimization of the process, the following conditions were used:

- Minimization of oxidant concentration
- Minimization of Fe^{2+} concentration
- Minimization of treatment time
- Oxidant type in range (H_2O_2 or $S_2O_8^{2-}$)

The following goals were selected for the responses:

- Maximization for COD removal
- Maximization for TSU removal

2.8. Kinetic study

The kinetics of H_2O_2 and $S_2O_8^{2-}$ were described mathematically, taking into account the reaction scheme presented in Table 5- The simplified reaction scheme was developed based on scavenging tests and several hypothesis from literature(Conte et al., 2012; Giménez et al., 2023; Pignatello et al., 2006; Simunovic et al., 2011), and it relies on the following assumptions:

i) The only oxidising species considered were $^{\bullet}OH$ for Fe^{2+}/H_2O_2 and $SO_4^{\bullet-}$ for $Fe^{2+}/S_2O_8^{2-}$;
ii) Radical-radical termination reactions were neglected compared to the propagation ones;
iii) The oxygen concentration is always in excess.

Then, these assumptions allowed to obtain the reaction rate expressions, for the studied species (Table 6).

The set of differential equations was solved using the MATLAB function "ode23s", and the model parameters were determined using the built-in optimization routine "lsqcurvefit" (Gualda-Alonso et al., 2022; Pontes et al., 2010).

3. Results and discussion

3.1. Preliminary FF and fenton processes optimization on synthetic LGW

In this work, the Fenton processes Fe^{2+}/H_2O_2 and $Fe^{2+}/S_2O_8^{2-}$ were optimized using RSM analysis to evaluate their potential as post-treatment of FF process in LGW treatment. Firstly, the FF process was applied to synthetic LGW to remove COD (based on optimal conditions determined in a previous work (Faggiano et al., 2022)) and, for the first time, to remove TSU. The goal of FF process was to efficiently and rapidly reduce both the organic and inorganic matter (in terms of COD) as well as surfactants (measured as TSU). The FF process demonstrated significant removal efficiencies for both parameters investigated. Specifically, after 120 min of treatment with an air flow of 3 L/min, the COD of raw LGW was reduced from 650 ± 35 mg/L to 140 ± 15 mg/L, representing a percentage reduction of 78.4 ± 1.5%. Similarly, the TSU initial concentration decreased from 58.7 ± 1.1 mg/L to 8.5 ± 1.4 mg/L resulting in a removal efficiency of 85.5 ± 2.1% after 120 min of treatment, with an air flow of 3 L/min. Considering that COD and TSU are challenging parameters to remove in LGWs, the excellent achieved through FF process motivated the subsequent optimization of the Fenton processes using RSM. The objective was tom achieve effluent conditions suitable for reuse. Based on the results obtained from the quadratic model, the empirical relationships between the response and the independent variables can be described by the following equations (Eq. 3 and Eq. (4)):

$$Y_{COD} = 78.03 + 1.960X_1 - 3.088X_2 + 4.612X_3 + 2.043X_4 + 6.894X_1X_2 + 4.722X_1X_3 + -4.990X_1X_4 - 1.443X_2X_3 + 7.364X_2X_4 - 1.534X_3X_4 + 2.140{X_1}^2 - 10.29{X_2}^2 - 14.82{X_3}^2 \quad \text{Eq. 3}$$

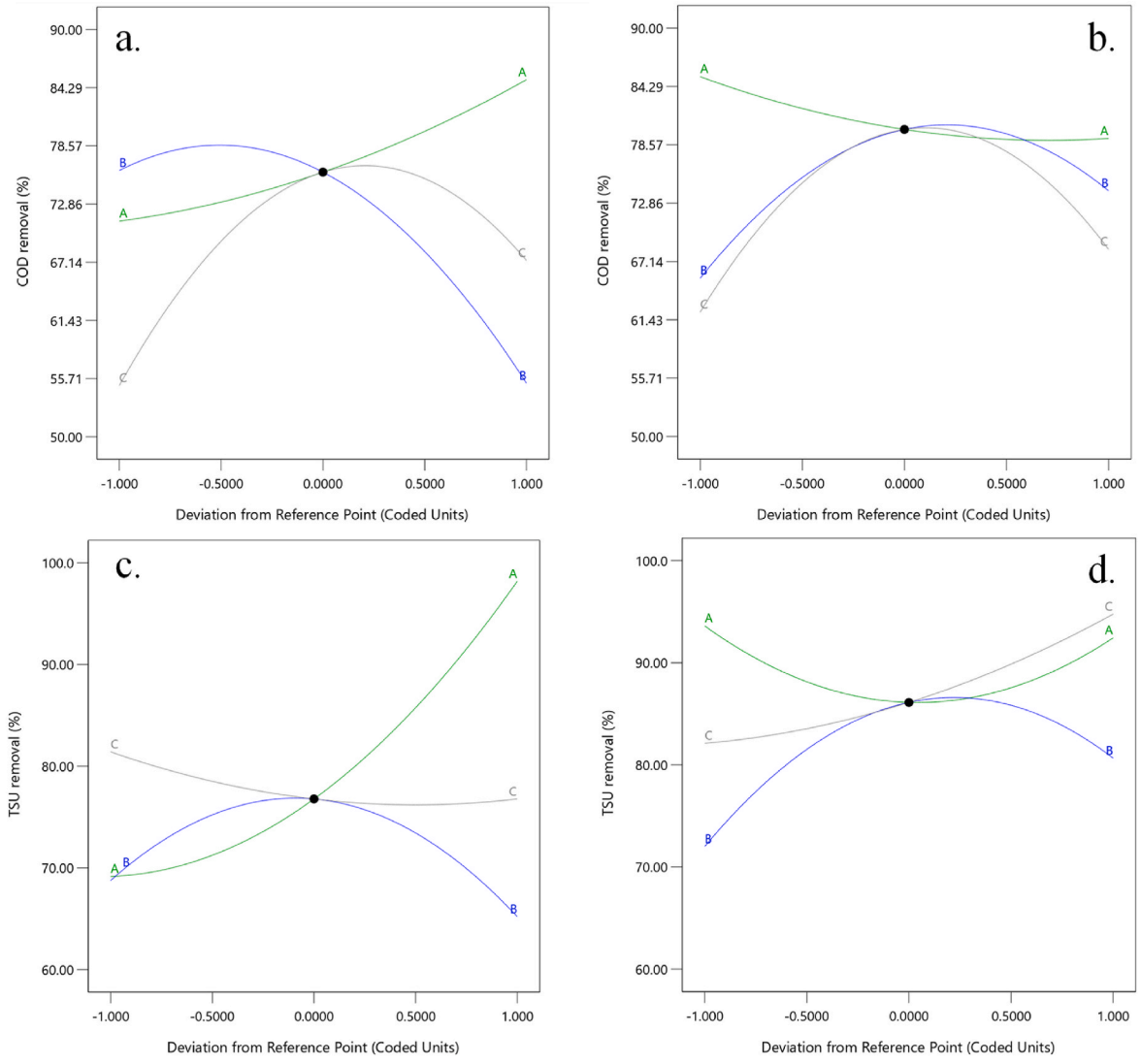

Fig. 2. Perturbation plots for COD removal with H_2O_2 (a) and $S_2O_8^{2-}$ (b) as oxidant and TSU removal with H_2O_2 (c) and $S_2O_8^{2-}$ (d) as oxidant. A, B and C represent Fe^{2+} concentration, oxidant dose and treatment time respectively.

$$Y_{TSU} = 81.45 + 6.965X_1 + 1.270X_2 + 2.008X_3 + 4.676X_4 - 0.5643X_1X_2 + 5.687X_1X_3 + \\ -7.547X_1X_4 - 3.731X_2X_3 + 3.052X_2X_4 + 4.321X_3X_4 + 6.902{X_1}^2 - 9.790{X_2}^2 + 2.316{X_3}^2 \quad \text{Eq. 4}$$

The results of the ANOVA for COD and TSU removals have been reported and thoroughly discussed in the Supporting Materials (SM) file. In summary, the determination coefficients for COD and TSU removals were $R^2 = 0.9843$ and $R^2 = 0.9889$, respectively. The differences between predicted and adjusted R^2 were less than 0.2 in both cases. Importantly, the Lack of Fit tests for both COD removal (p-value: 0.9588) and TSU removal (p-value: 0.5039) were not significant compared to pure error.

Concerning the validation of the model assumptions, the residual plots shown in SM file demonstrate small deviation from the straight line. This indicates that the studentized residuals can be considered to follow a normal distribution both for COD and TSU removals. The residual plots display a random scatter approximately centred on zero across the entire range of predicted values, indicating that the residuals are random and the variance of the observations is constant for all response values (Ribeiro et al., 2020, 2020, 2020). Moreover, no outliers were identified in either case.

The removals of COD and TSU were investigated under different operating conditions as suggested by the experimental RSM design. Fig. 2 displays the perturbation plots for COD and TSU removal. In these plots, the iron concentration (A), oxidant concentration (B) and treatment time (C) are plotted to compare their effects at a particular point in the design space. How the responses change as each factor moves away from the reference point (which, in this study, is the midpoint). On the x-axis, −1, 0, and +1 represent the lower, middle, and upper levels of the investigated factors, respectively. In the discussion of perturbation plots, a positive effect means that the response increases with the increment of the factor level, while a negative effect suggest that response decreases

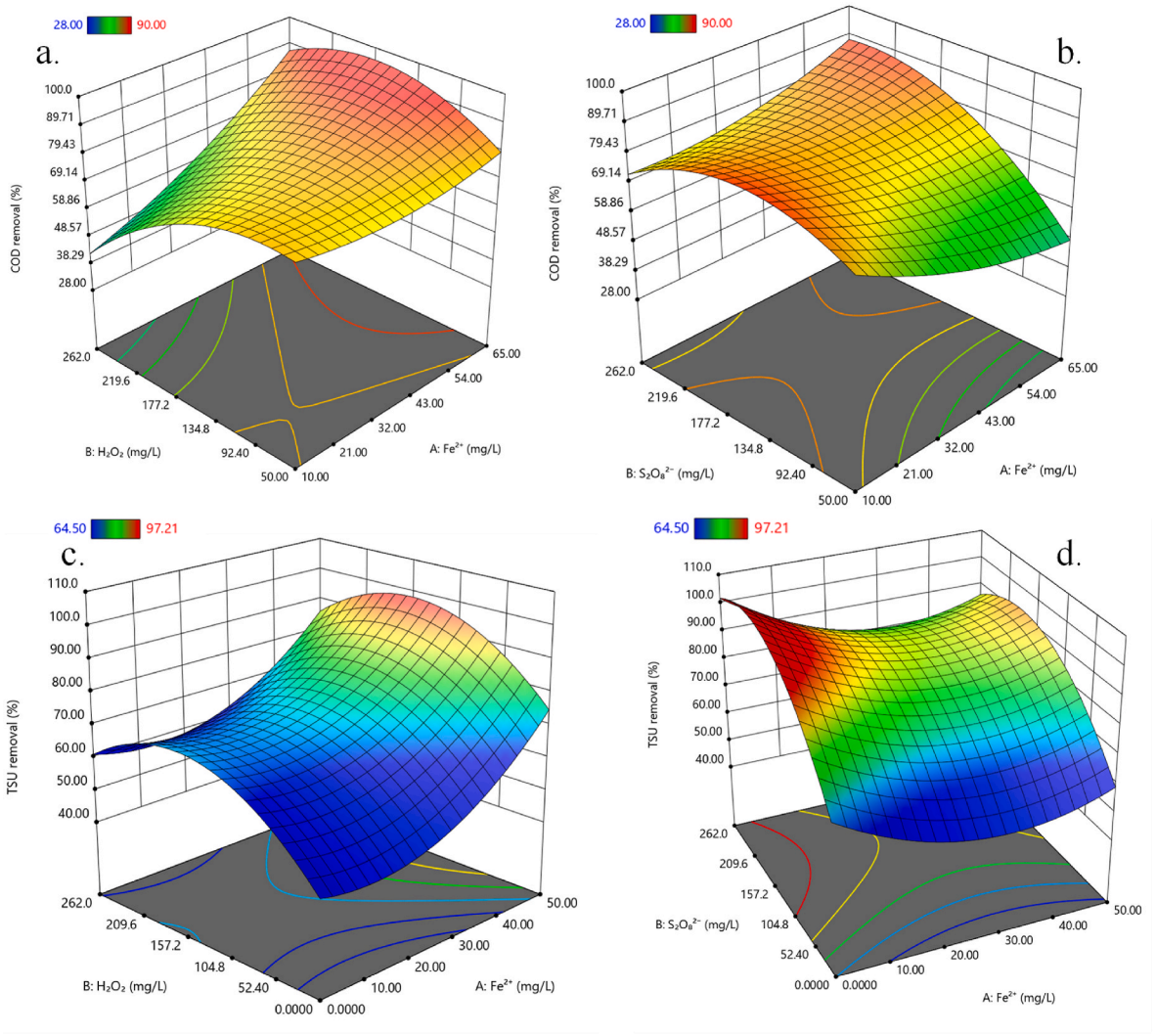

Fig. 3. Response plots for COD removal with H_2O_2 (a) and $S_2O_8^{2-}$ (b) as oxidant and TSU removal with H_2O_2 (c) and $S_2O_8^{2-}$ (d) as oxidant in 30 min of treatment time.

due to the increase in the factor level.

Regarding COD removal, oxidant dosage and treatment time initially showed a positive effect until reach the midpoint, after which a negative effect was observed. On the other hand, Fe^{2+} dosage, showed two opposite trends. When H_2O_2 (Fig. 2a) was tested as the oxidant agent, Fe^{2+} has a positive effect. However, when it was replaced with $S_2O_8^{2-}$ (Fig. 2b), Fe^{2+} had a negative effect. This clearly indicates that $S_2O_8^{2-}$ requires much lower concentrations of Fe^{2+} to be activated, in contrast to H_2O_2 which requires high concentrations. This represents a significant environmental advantage as Fe^{2+} in Fenton processes not only participates as an oxidant activator but is also the main actor in the coagulation process. When TSU removal efficiency was evaluated, Fe^{2+} concentration exhibited a strong positive effect (Fig. 2c), while H_2O_2 concentration showed a concave effect (similar to that shown in COD removal). Treatment time had a relatively constant effect, with only a slight, insignificant decrease in efficiency observed with increasing treatment time. When H_2O_2 was replaced with $S_2O_8^{2-}$, Fe^{2+} concentration had a slightly negative effect until midpoint and after which it had a slightly positive effect. $S_2O_8^{2-}$ concentration exhibited a positive effect until midpoint and then a negative one while treatment time showed a positive effect. It is important to note that in TSU removal, the highest efficiencies are achieved at either low or high Fe^{2+} concentrations. This is justified by the fact that when the Fe^{2+} concentration is low, it is nevertheless appropriate to activate the $S_2O_8^{2-}$ by generating an oxidation process. When the Fe^{2+} concentration is high, it is the coagulation process that is prevalent, so in environmental terms for the same efficiency the more inappropriate process is triggered. Two and three-dimensional response surfaces of the quadratic model were utilized to assess the interactions between independent variables and responses. In these analyses, two variables were held constant while the others varied within the experimental ranges. The three-dimensional response surface of COD and TSU removal efficiencies are shown in Fig. 3.

The Fe^{2+}/H_2O_2 system achieved a maximum COD removal efficiency of approximately 72% using Fe^{2+} and H_2O_2 concentrations of 50 mg/L and 65.5 mg/L, respectively, with a treatment time of 30 min, On the other hand, the Fe2+/S2O82- system reached a maximum COD removal efficiency of about 77%with Fe^{2+} and $S_2O_8^{2-}$ concentrations of 25 mg/L and 262 mg/L, respectively, in a treatment time of 45 min. In terms of TSU removal, the Fe^{2+}/H_2O_2 system achieved a maximum efficiency of approximately 88% under the same operating conditions as the COD removal. Conversely, the $Fe^{2+}/S_2O_8^{2-}$ system achieved about 97% TSU removal with Fe^{2+} and $S_2O_8^{2-}$ concentrations of 12.5 mg/L and 196.5 mg/L, respectively. From the surface analysis, it can be concluded that $S_2O_8^{2-}$ achieves higher removal rates for both COD and TSU. Moreover, oxidative processes require low oxidant concentrations but higher Fe^{2+} concentrations in Fe^{2+}/H_2O_2, as opposed to $Fe^{2+}/S_2O_8^{2-}$, which requires higher oxidant concentrations but lower Fe^{2+} concentrations. To the best of the authors' knowledge, the conventional Fenton process has not

Table 7
Change in COD and TSU removal efficiencies in the switch form synthetic to real LGW.

Parameter	Removal in synthetic LGW (%)	Removal in real LGW (%)
Fe^{2+}/H_2O_2 process		
COD	88 ± 4	78 ± 8
TSU	88.2 ± 2.5	96.6 ± 4.5
$Fe^{2+}/S_2O_8^{2-}$ process		
COD	93 ± 2	89 ± 3
TSU	97.1 ± 0.8	99.7 ± 1.3

been previously studied using RSM as a post-treatment to a physical process in the treatment of GW. In the literature, electro-Fenton is one of the most extensively studied processes for treating GW, as reported in a recent work (dos Santos et al., 2023), which discusses the main treatment processes studied for GW. Specifically, in the study by dos Santos et al. (dos Santos et al., 2023), a 50% and 70% removal efficiency for COD (about 250 mg/L of initial concentration) and ASU (about 2.5 mg/L of initial concentration) was reached by solar photo-electro Fenton after 240 min. The initial COD compared to our work is comparable (250 vs 150 mg/L), while the initial concentration of ASU is much higher in our work (2.5 vs 58 mg/L). From the results obtained in this study, the Fenton process utilizing $S_2O_8^{2-}$ shows promising potential for the treatment of GW.

3.2. Process optimization and kinetics on real LGW

3.2.1. Organic matter, nutrients and surfactants removal

According to the RSM analysis, the optimal conditions for effectively removing COD and TSU in Fenton processes, using both $S_2O_8^{2-}$ ad H_2O_2, are as follows:

i) 12.5 mg/L of Fe^{2+}, 185.6 mg/L of $S_2O_8^{2-}$, 30 min of treatment time
ii) 50 mg/L of Fe^{2+}, 157.6 mg/L of H_2O_2, 30 min of treatment time

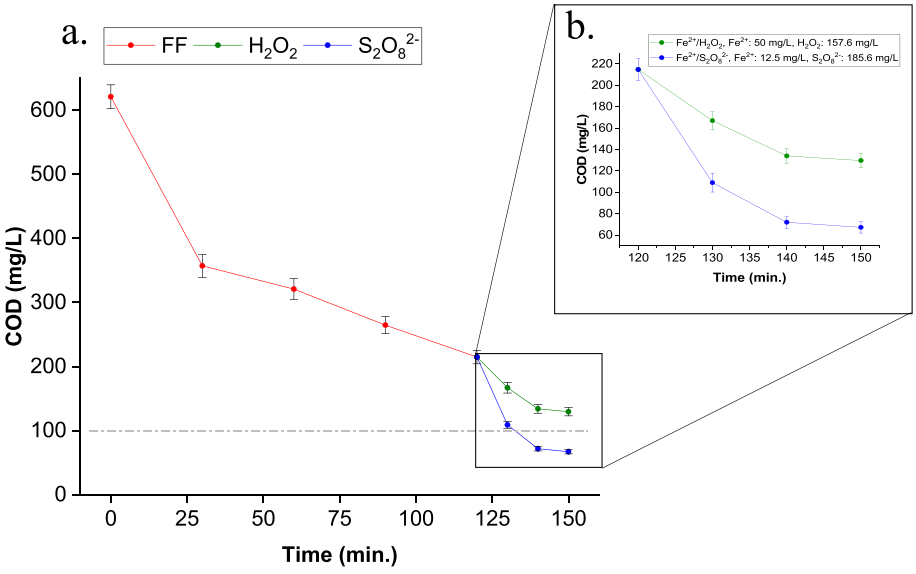

Fig. 4. COD removal by FF (until 120 min) (a) followed by Fe^{2+}/H_2O_2 (green line) or $Fe^{2+}/S_2O_8^{2-}$ (blue line) (b) (between 120 and 150 min). (For interpretation of the references to colour in this figure legend, the reader is referred to the Web version of this article.)

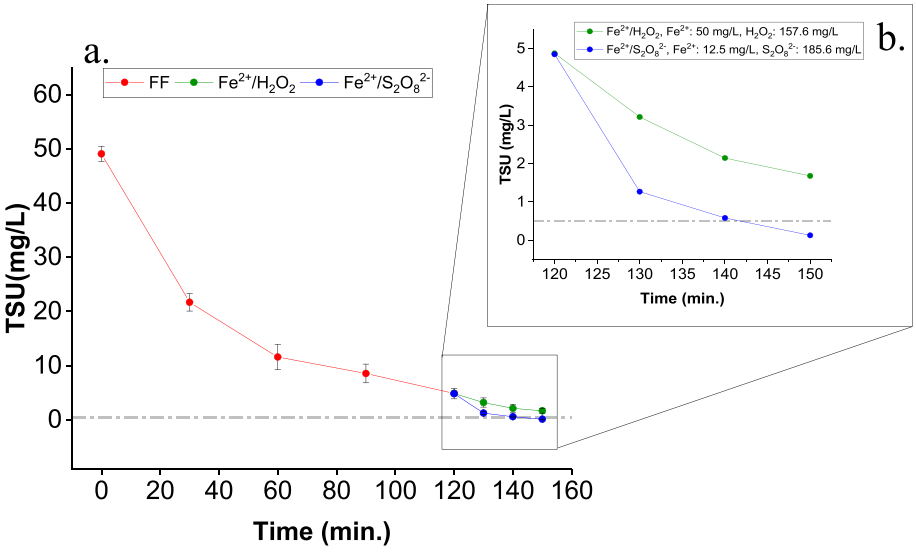

Fig. 5. TSU removal by FF (until 120 min) (a) followed by Fe^{2+}/H_2O_2 (green line) or $Fe^{2+}/S_2O_8^{2-}$ (blue line) (b) (between 120 and 150 min). (For interpretation of the references to colour in this figure legend, the reader is referred to the Web version of this article.)

Table 8
GW parameter before and after Fe^{2+}/H_2O_2 and $Fe^{2+}/S_2O_8^{2-}$ processes.

Parameter	Raw LGW (mg/L)	After Fe^{2+}/H_2O_2	After $Fe^{2+}/S_2O_8^{2-}$
COD	600 ± 28	130 ± 8	67 ± 6
BOD_5	85 ± 15	15 ± 4	6 ± 2
TN	16 ± 4	2.3 ± 0.6	3.4 ± 0.7
TP	7 ± 2	1.4 ± 0.3	2.1 ± 0.3
ASU	43.4 ± 0.3	1.66 ± 0.1	0.13 ± 0.01
NISU	5.7 ± 0.2	0.016 ± 0.003	0.002 ± 0.001
TSU	49.1 ± 0.5	1.68 ± 0.1	0.13 ± 0.01

These optimal conditions were applied to real LGW to evaluate COD, BOD_5, TSU, TN and TP reduction as well as disinfection, which will be discussed in the next paragraph. In the transition from synthetic to real GW, COD varied from 650 ± 35 mg/L to 600 ± 88 mg/L while TSU varied from 58.7 ± 1.1 mg/L to 49.1 ± 0.5 mg/L. Specifically, the ASU concentration varied from 50.3 ± 0.4 mg/L to 43.4 ± 0.3 mg/L, NISU from 8.1 ± 0.6 mg/L to 5.7 ± 0.2 mg/L for synthetic and real GW respectively was not detected in real LGW. When the real LGW were tested, the COD removal efficiency decreased from 93 ± 2% to 89 ± 3% and from 88 ± 4% to 78 ± 8% for $Fe^{2+}/S_2O_8^{2-}$ and Fe^{2+}/H_2O_2 process respectively. TSU removal changed from 97.1 ± 0.8% to 99.7 ± 1.3% and from 88.2 ± 2.5% to 96.6 ± 4.5% for $Fe^{2+}/S_2O_8^{2-}$ and Fe^{2+}/H_2O_2 process respectively. Percentage removals of COD and TSU with $Fe^{2+}/S_2O_8^{2-}$ process were very similar in the passage from synthetic LGW to real LGW, while for Fe^{2+}/H_2O_2 higher differences were detected both in COD and TSU removal. However, when Fe^{2+}/H_2O_2 was applied, the standard deviations and removal efficiencies were higher, likely due to the high Fe^{2+} concentration which also generates a coagulation process that is less selective than the oxidation process. The differences between synthetic and real LGW are summarized in Table 7.

The optimized in significant COD removal percentages (Fig. 4). Specifically, pre-treatment with FF achieved 60 ± 1% of COD removal (with a final COD value of 241 ± 10 mg/L). As can be seen from Fig. 4, during the first 60 min of treatment, foam formation substantial and rapid, leading to approximately 45 ± 1% removal. This result is in agreement with another work (Faggiano et al., 2022) where COD removal was analyzed by FF with a COD reduction on synthetic GW matrix of approximately 72%. In this current work, after 120 min, a COD reduction of about 60 ± 1% was reached in real LGW.

Considering the stringent limits for wastewater reuse imposed by different Countries, these performances in terms of COD removal, may not be sufficient to meet the respective standards, making the subsequent polishing step necessary. In fact, a value below 100 mg/L is required in many countries for DWW reuse. The Fenton processes using Fe^{2+}/H_2O_2 and $Fe^{2+}/S_2O_8^{2-}$ were subsequently tested as post-treatments to comply with the regulatory limit. Specifically, both processes allowed to reduce COD already in the first 5 min of treatment (Fig. 4b) by a good percentage, however, the Fe^{2+}/H_2O_2 process reaches a plateau after 10 min, and does not allow it to fall below the regulatory limit, with a residual COD value of 130 ± 8 mg/L. The $Fe^{2+}/S_2O_8^{2-}$ process allows for higher efficiencies to be achieved. After just 5 min, the COD value is close to the regulatory limit, and after 30 min, the residual COD value falls to 67 ± 6 mg/L, which is below the regulatory limits. In terms of TSU removal (Fig. 5), the FF process achieved a maximum removal of 85 ± 2% after 120 min. Similarly, to the COD removal, a good removal percentage was obtained after only 60 min of treatment with a value of about 76 ± 3%. However, the final TSU concentration (7.25 ± 0.5 mg/L) exceeds the regulatory limits.

After the FF process, the optimized Fe^{2+}/H_2O_2 and $Fe^{2+}/S_2O_8^{2-}$ processes were implemented to assess the potential for achieving effluent quality suitable for reuse. With Fe^{2+}/H_2O_2, a residual TSU concentration of 1.68 ± 0.1 mg/L was obtained, which, similar to COD, exceeds the regulatory limit (0.5 mg/L of TSU for Italy regulation and 0.2 mg/L of ASU for Australia regulation). The $Fe^{2+}/S_2O_8^{2-}$ process, on the other hand, enables the TSU value to drop below the regulatory limit for both mentioned regulation (final value of 0.13 ± 0.01 mg/L). In fact, after 20 min of treatment, the TSU value approaches the regulatory limit, and after 30 min it falls below the limit. The greater removal percentages of COD, BOD_5 and TSU achieved with $Fe^{2+}/S_2O_8^{2-}$ process compared to Fe^{2+}/H_2O_2 process are attributed to the higher activity of $SO_4^{-\bullet}$ radical compared to $^{\bullet}OH$. This is primarily due to the higher reduction potential of $SO_4^{-\bullet}$ (2.5–3.1 V) compared to $^{\bullet}OH$ (1.8–2.7 V) and its longer half-life period ($t_{1/2}$ = 30–40 μs versus 20 ns) (Arellano et al., 2019; Ghanbari and Moradi, 2017). Graphs of ASU and NISU removals under the same conditions are presented in the Supplementary material (SM) file (Fig. SM1 and Fig. SM2 respectively). The final values of BOD_5, TN, TP, NISU and ASU are provided in Table 8. Residual oxidant concentrations after Fe^{2+}/H_2O_2 and $Fe^{2+}/S_2O_8^{2-}$ processes were 0.13 mg/L and 0.09 mg/L respectively. Graph of oxidant consumption throughout the AOPs are shown in SM file (Fig. SM5). Following the optimized $Fe^{2+}/S_2O_8^{2-}$ process, SO_4^{2-} concentration was evaluated to

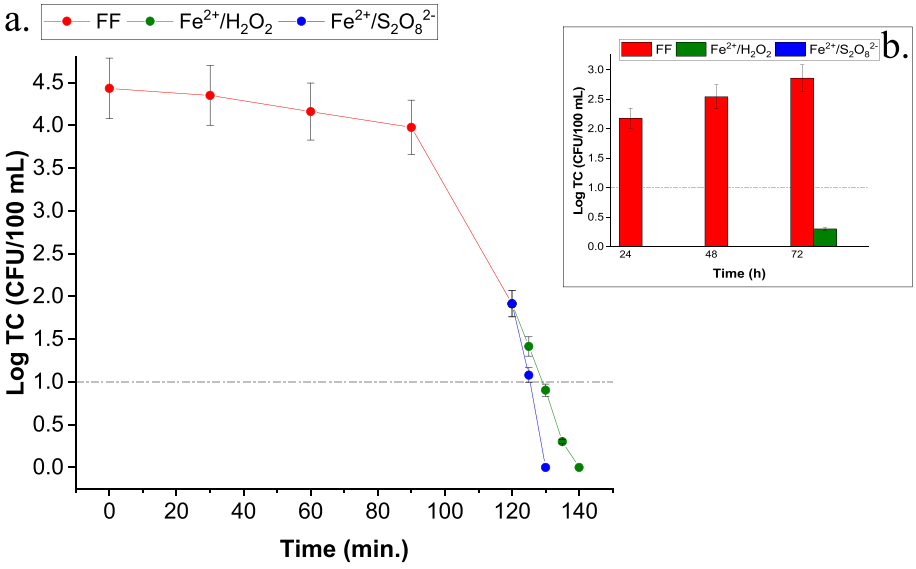

Fig. 6. TC removal by FF (until 120 min) followed by Fe^{2+}/H_2O_2 (green line) or $Fe^{2+}/S_2O_8^{2-}$ (blue line) (between 120 and 150 min) (a). TC regrowth after FF (red bar), Fe^{2+}/H_2O_2 (green bar) and $Fe^{2+}/S_2O_8^{2-}$ (blue bar) (b). In Fe^{2+}/H_2O_2 process, Fe^{2+}: 50 mg/L and H_2O_2: 157.6 mg/L. In $Fe^{2+}/S_2O_8^{2-}$, Fe^{2+}: 12.5 mg/L and $S_2O_8^{2-}$: 187.6 mg/L. (For interpretation of the references to colour in this figure legend, the reader is referred to the Web version of this article.)

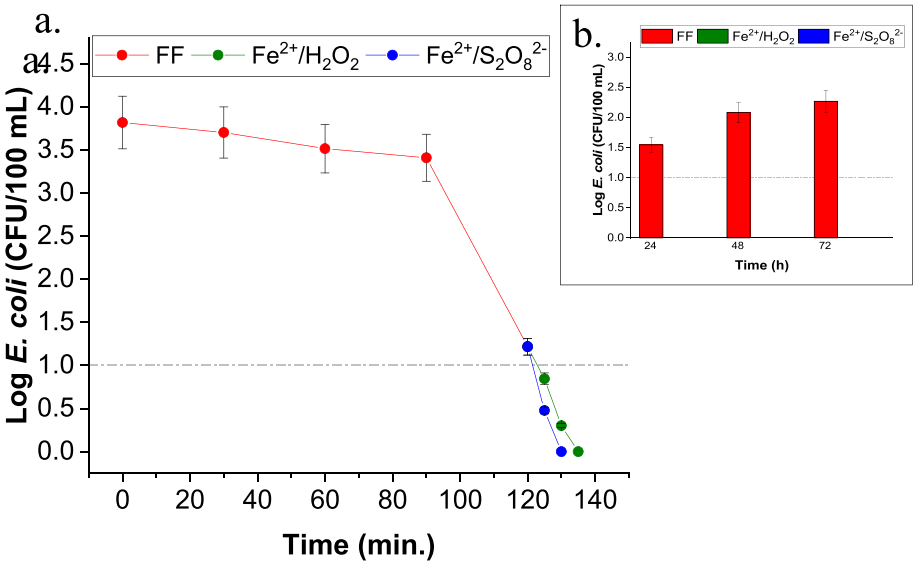

Fig. 7. E. coli removal by FF (until 120 min) followed by Fe^{2+}/H_2O_2 (green line) or $Fe^{2+}/S_2O_8^{2-}$ (blue line) (between 120 and 150 min) (a). E. coli regrowth after FF (red bar), Fe^{2+}/H_2O_2 (green bar) and $Fe^{2+}/S_2O_8^{2-}$ (blue bar) (b). In Fe^{2+}/H_2O_2 process, Fe^{2+}: 50 mg/L and H_2O_2: 157.6 mg/L. In $Fe^{2+}/S_2O_8^{2-}$, Fe^{2+}: 12.5 mg/L and $S_2O_8^{2-}$: 187.6 mg/L. (For interpretation of the references to colour in this figure legend, the reader is referred to the Web version of this article.)

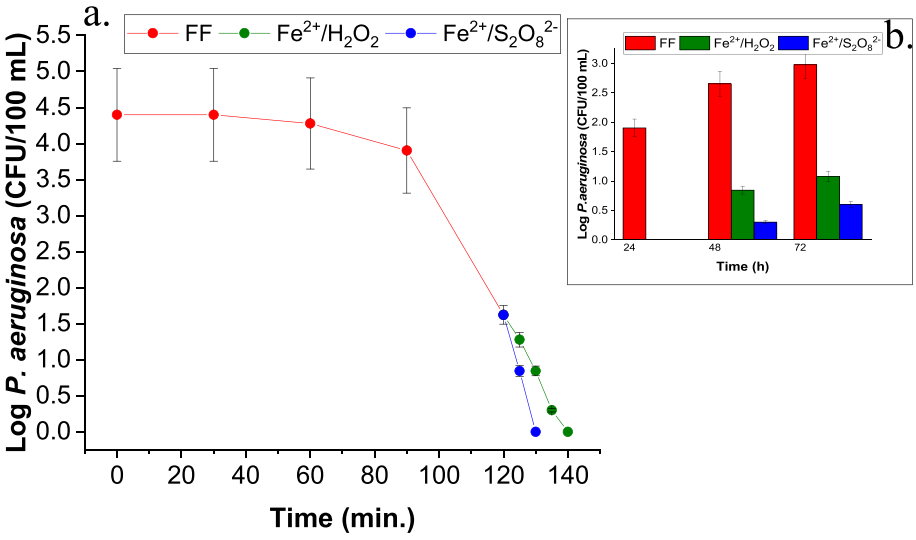

Fig. 8. P. aeruginosa removal by FF (until 120 min) followed by Fe^{2+}/H_2O_2 (green line) or $Fe^{2+}/S_2O_8^{2-}$ (blue line) (between 120 and 150 min) (a). P. aeruginosa regrowth after FF (red bar), Fe^{2+}/H_2O_2 (green bar) and $Fe^{2+}/S_2O_8^{2-}$ (blue bar) (b). In Fe^{2+}/H_2O_2 process, Fe^{2+}: 50 mg/L and H_2O_2: 157.6 mg/L. In $Fe^{2+}/S_2O_8^{2-}$, Fe^{2+}: 12.5 mg/L and $S_2O_8^{2-}$: 187.6 mg/L. (For interpretation of the references to colour in this figure legend, the reader is referred to the Web version of this article.)

assess the effluent quality for discharge. A maximum concentration of 128 mg/L of SO_4^{2-} was observed. This concentration is below the Italian regulatory limits (1000 mg/L for discharge in superficial water and 500 mg/L for water reuse) (Decreto Legislativo 152/06 "Norme in materia ambientale," 2006).

As evident from Table 8, the entire process achieved significant removals of BOD_5, TN and TP. Specifically, removals of 82 ± 1%, 86 ± 1% and 80 ± 2% were reached for BOD_5, TN and TP respectively with the FF followed by Fe^{2+}/H_2O_2 process. Removals equal to 93 ± 1%, 79 ± 1% and 70 ± 4% were reached for BOD_5, TN and TP respectively with the FF followed by $Fe^{2+}/S_2O_8^{2-}$ process. After the Fenton processes, sludge production was 1.9 ± 0.3 mL/L and 0.4 ± 0.2 mL/L for Fe^{2+}/H_2O_2 and $Fe^{2+}/S_2O_8^{2-}$ respectively. The variation in sludge volume between the two processes can be attributed to the different dosage of Fe^{2+} required under the optimized conditions for each oxidant agent. In particular, 50 mg/L and 12.5 mg/L were used for Fe^{2+}/H_2O_2 and $Fe^{2+}/S_2O_8^{2-}$ respectively. Additionally, the higher removal efficiencies obtained wit $Fe^{2+}/S_2O_8^{2-}$ in terms of organic matter and surfactants concentration does not affect sludge production, as shown in perturbation plots (Fig. 2), because for both Fenton processes the oxidation process is prevalent on coagulation one. Therefore, sludge production, under these experimental conditions, is strictly and exclusively related to the initial Fe^{2+} concentration. Other recent studies investigated COD removal in real GW by chemical, electro-chemical and photo-electro chemical processes. A limited COD (initial concentration ranged between 600 and 700 mg/L) removal of 50%, compared to this work, was obtained with a multi-barrier system consisting of several step of ultrafiltration, adsorption and electrocoagulation/electrooxidation in a treatment time of 120 min (Khosravanipour Mostafazadeh et al., 2019). Ghanbari et al. (Ghanbari and Moradi, 2017) investigated the application of electro-Fenton with 300 mg/L of HSO_5^-, 100 mg/L of iron nanoparticles as catalyst and a current of 30 mA in a treatment time of 180 min

reaching a COD removal of about 99% (initial COD concentration of 480 mg/L. Although the COD removal is higher than that obtained by us in this work, electro-Fenton which is a COD removal higher than that obtained in this work but required 30 min longer time of treatment, a higher oxidant concentration and the constant use of electric energy. The removal of ASU with AOPs was investigated by Teodoro et al., 2014 (Teodoro et al., 2014) through the application of Fe^{2+}/H_2O_2 at pH 3 with 10 mg/L of Fe^{2+} and 150 mg/L of H_2O_2. They observed a percentage removal of ASU of 99% (initial concentration of about 25 mg/L) in a longer treatment time (120 min) and the process was assisted by UVC radiation. Dos Santos et al. (dos Santos et al., 2023) also investigated the removal of ASU (initial concentration of about 2.5 mg/L) through anodic oxidation with H_2O_2 as oxidant reaching 84% after 240 min of treatment time, however, the process they investigate requires continuous use of electricity

3.2.2. Disinfection and regrowth tests

Optimized FF followed by Fe^{2+}/H_2O_2 and FF followed by $Fe^{2+}/S_2O_8^{2-}$ processes were evaluated also in the removal of *TC* (Fig. 6), *E. coli* (Fig. 7) and *P. aeruginosa* (Fig. 8) and regrowth after 24, 48 and 72 h of real LGW. For the first time FF process was investigated in disinfection of GW. For all three investigated species, FF achieved a bacterial removal of approximately 3 Log units. In each case the bacterial removal trend is very similar, with low removals until 90 min, about 0.5 Log units for *TC* and *P. aeruginosa* and a little bit less than 0.3 Log units for *E. coli.* A significant increase in bacterial removal was observed during the last 30 min, specifically between 90 and 120 min, for each bacterial species investigated. Approximately 2.5 Log units of removal was detected for all three species. This notable decrease observed at the end of the FF process may be attributed to the high concentration of surfactants in real LGW, which exceeds the critical micellar concentration. In this way, at the beginning of the process surfactants are assembled in micelles which are more stable than free surfactants alone and the interaction with bacterial membranes is very limited. As the insufflation time increases (especially after 60 min) a flotation of free soap particles can be observed. Bacteria and viruses have lipid membranes that resemble double-layered micelles but with a double lipid layer, therefore the hydrophobic tails of the free-floating soap molecules can wedge themselves into the lipid envelopes of certain microbes and viruses, prying them apart from the matrix. The optimized Fenton processes demonstrated highly rapid bacterial removal. Specifically, with Fe $^{2+}/H_2O_2$ (50 mg/L of Fe^{2+} and 157.6 mg/L of H_2O_2), complete inactivation of TC (Fig. 6a), E. coli (Fig. 7a), and P. aeruginosa (Fig. 8a) was observed within 15 mi. However, after 10 and 5 min the bacterial concentration was below the regulatory limit for *TC* and *E. coli* respectively. $Fe^{2+}/S_2O_8^{2-}$ process (12.5 mg/L of Fe^{2+} and 185.2 mg/L of $S_2O_8^{2-}$) exhibited even faster removal kinetics, achieving complete inactivation of TC, E. coli, and P. aeruginosa within 10 min while a bacterial concentration below the regulatory limit was reached in about 5 min.

Substantial bacterial regrowth was detected for all three bacterial families after FF, which was an expected finding, as there was no total removal after FF. In particular, a minor regrowth was observed after 24 h (<0.5 Log units), followed by an increase of approximately 1 Log unit between 24 and 72 h. No regrowth was observed for *E. coli* in both Fenton processes, while a regrowth of a few colonies of *TC* was detected after 72h in the Fe^{2+}/H_2O_2 process. In contrast, regrowth of *P. aeruginosa* was observed at 48 and 72 h for both Fenton processes, in fact in the case of $Fe^{2+}/S_2O_8^{2-}$ the regrowth was about 0.5 log units, whereas in the case of Fe^{2+}/H_2O_2 the regrowth at 72 h was about 1 log unit. Bacterial disinfection in Fenton's processes is due to the action of radicals causing intra- and extracellular damage (O'Dowd and Pillai, 2020). Teodoro et al. (2018)(Teodoro et al., 2018) investigated the removal of *P. aeruginosa* with Fenton and Photo-Fenton processes in GW. In their case, inactivation of 5 Log Units of *P. aeruginosa* were achieved in about 20 min (thus very similar to this work) with H_2O_2 concentrations of 150 mg/L and Fe^{2+} concentrations of 10 mg/L by Fenton

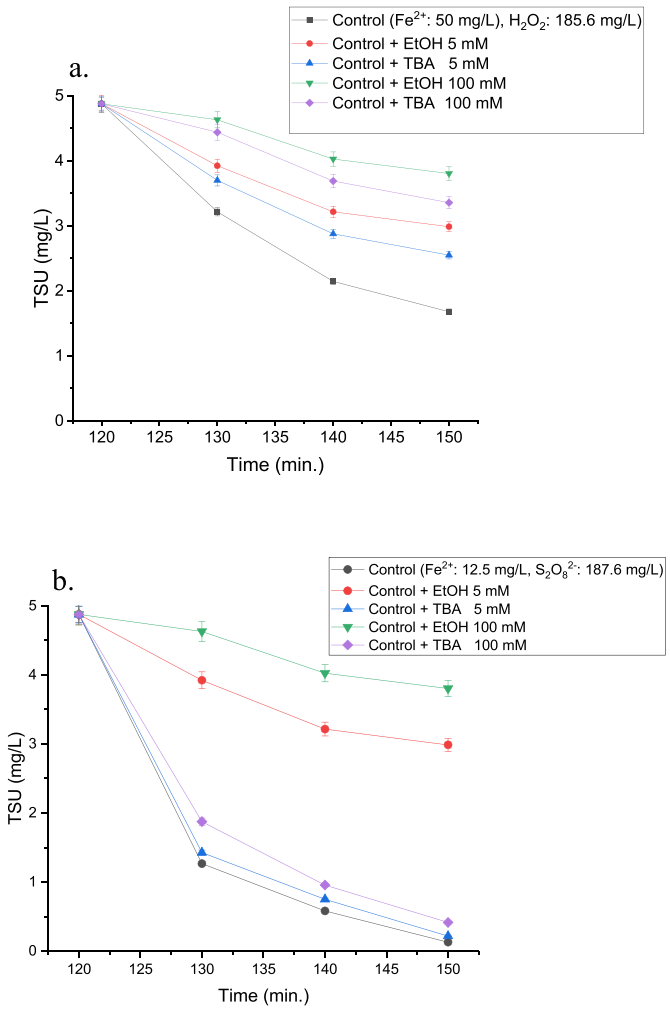

Fig. 9. Rates of TSU degradation in the presence of quenching agents for Fe^{2+}/H_2O_2 (a) and $Fe^{2+}/S_2O_8^{2-}$ (b) processes.

process. However, in their case, the COD concentration was considerably lower (around 80 mg/L versus around 240 mg/L). Therefore, a 3-fold lower COD concentration achieved similar inactivation kinetics but with less iron, as the presence of organic matter strongly influences the activity of radicals, reducing their availability to the disinfection process(Zhou, 2017). Moreover, Teodoro et al. (2018)(Teodoro et al., 2018) also investigated photo-Fenton processes on *P. aeruginosa* removal and regrowth after 24 h and coherently with our work no regrowth was detected after this time. Although there are few studies on bacterial removal in GW, it is interesting to note that in many studies on DWW, Fenton processes have been coupled with solar radiation in order to decrease iron concentration or to make the processes faster(Abeledo--Lameiro et al., 2019; Zapata et al., 2009). In this study, by applying RSM, the optimal Fenton concentrations for the two investigated processes were determined. It was observed that the $Fe^{2+}/S_2O_8^{2-}$ process achieves faster bacterial removal than Fe^{2+}/H_2O_2, despite using Fe concentrations that are 5 times lower. Thus, the $Fe^{2+}/S_2O_8^{2-}$ process shows great promise for GW disinfection since Fe^{2+} effectively activates $S_2O_8^{2-}$ (Karim et al., 2021; Liu et al., 2012). Consequently, even at low concentrations of Fe^{2+} in the solution, a significant amount of $SO_4^{\bullet-}$ radicals is generates (with a considerably longer half-life than $^{\bullet}OH$).

3.3. Identification of predominate radical species

Radical inhibition experiments were conducted to identify the dominant radical oxidant ($SO_4^{\bullet-}$ vs. $^{\bullet}OH$) by observing the differences in

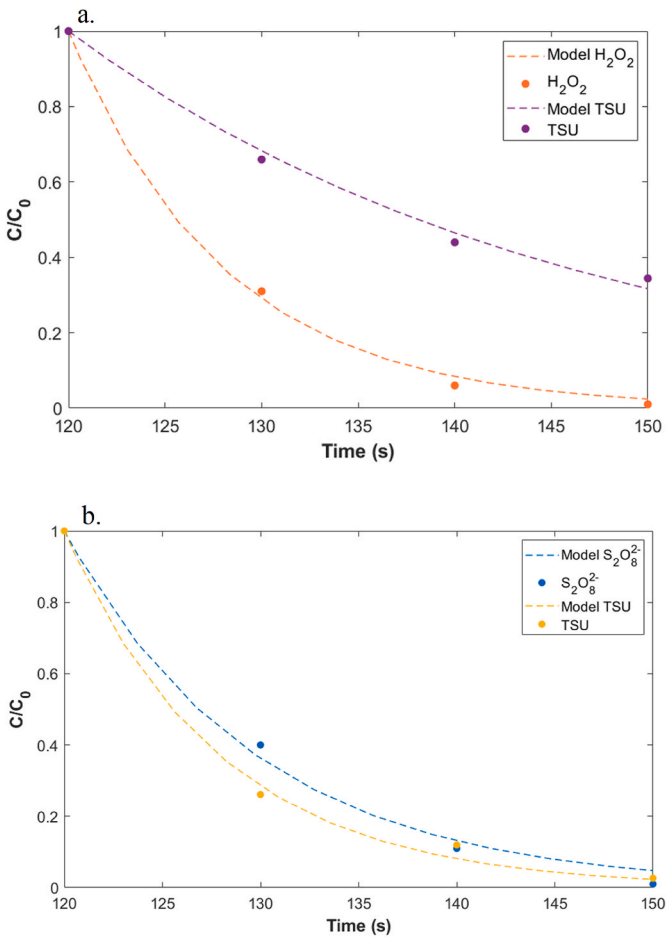

Fig. 10. Experimental and model results for H_2O_2, $S_2O_8^{2-}$ and TSU, in relative concentrations. a) $[Fe^{2+}]_0$ = 50 mg/L, $[H_2O_2]_0$ = 157.6 mg/L, b) $[Fe^{2+}]_0$ = 12.5 mg/L, $[S_2O_8^{2-}]_0$ = 185.6 mg/L.

radical reactivity toward two different alcohol additives, ethanol (EtOH) and tert-butyl alcohol (TBA) as carried out in previous work (Lin et al., 2015). The reaction of $SO4^{\cdot-}$ with TBA is reported to be considerably slower (4–9.1 × 10^5 M^{-1} s^{-1}) than that with EtOH (1.6–7.7 × 108 M^{-1} s^{-1}). The ·OH reacts rapidly even with EtOH and TBA. Therefore, EtOH is an effective quencher for both $SO4^{\cdot-}$ and ·OH, while TBA is an effective quencher for ·OH but not for $SO4^{\cdot-}$ (Lin et al., 2015). In particular, the scavenging test were performed on TSU degradation for both processes (Fe^{2+}/H_2O_2 and $Fe^{2+}/S_2O_8^{2-}$) to avoid interference of EtOH and TBA in COD measurement. 5 mM and 100 mM of each alcohol were tested (Fig. 9).

Fig. 9 shows the rate of TSU degradation in the presence of quenching reagents. With 5 and 100 mM of EtOH, the catalytic activity towards TSU degradation, was highly inhibited for both processes. However, TBA addition influenced drastically only the Fe^{2+}/H_2O_2 process. This result suggested that the dominant radical formed in $Fe^{2+}/S_2O_8^{2-}$ process was $SO4^{\cdot-}$. Hydroxy radicals might be also present in $Fe^{2+}/S_2O_8^{2-}$ process, but its contribution was very little compared with sulphate ones.

3.4. Kinetic study

The rate constant obtained for TSU degradation in the Fe^{2+}/H_2O_2 and $Fe^{2+}/S_2O_8^{2-}$ processes were k_5 = 0.0383 and k_9 = 0.1254 M^{-1} s^{-1} respectively. The low RMSE obtained for H_2O_2, $S_2O_8^{2-}$, TSU in the presence of H_2O_2 and TSU in the presence of $S_2O_8^{2-}$ (0.02, 0.04, 0.03 and 0.03 respectively) show that the kinetic model adequately describes the behaviour of the reacting system (Fig. 10)

4. Conclusions

This study proposed an efficient method for treating real GW through a combination of FF and $Fe^{2+}/S_2O_8^{2-}$ processes. This work investigated the removal of COD, TSU, *E. coli*, *P. aeruginosa* and *TC*.

The FF, a physical process which exploits the dual hydrophilic/hydrophobic properties of surfactants, was applied for the first time in the pre-treatment of real GW, allowing to obtain good organic matter, surfactants and bacterial removals. Approximately 60% and 76% removals of COD and TSU and more than 50% of bacterial load removal (*E. coli*, *TC* and *P. aeruginosa*) were reached after 120 min of treatment. The $Fe^{2+}/S_2O_8^{2-}$ and Fe^{2+}/H_2O_2 processes at pH = 3 were optimized through RSM analysis as post-treatment methods. $Fe^{2+}/S_2O_8^{2-}$ required 4 time less Fe^{2+} concentration and achieves higher removals for both COD and TSU, as well as faster bacterial removal compared to Fe^{2+}/H_2O_2. $Fe^{2+}/S_2O_8^{2-}$ process allows for compliance with the most stringent regulatory limits for wastewater reuse among the investigated parameters. Moreover, the $Fe^{2+}/S_2O_8^{2-}$ process results in significantly less sludge volume production compared to Fe^{2+}/H_2O_2 process. $Fe2^{+}/H_2O_2$ allowed to reach 78% and 96.6% of removal for COD and TSU respectively. With $Fe^{2+}/S_2O_8^{2-}$ process, instead, 89% and 99.7% of removal were obtained for COD and TSU respectively. The scavenging tests indicate the formation of ·OH radicals in the Fe^{2+}/H_2O_2 process, as expected, while the $Fe^{2+}/S_2O_8^{2-}$ process predominantly forms $SO_4^{\cdot-}$ radicals. Additionally, the kinetic model developed in this work confirms the main mechanisms of oxidising species and accurately describes the trend of the experimental data. The results achieved in this work make this technology promising and warrant further investigation, with potential applications in both developing and developed countries. Furthermore, the limited electricity consumption and reduced plant volumes align with the principles of low-carbon production and minimal land usage. The next steps in the research on this treatment for GWs should focus on critical points that may affects their reuse. Significant attention should be given to the presence of emerging contaminants such as antibiotics and antibiotic-resistant bacteria in GW, in order to study a treatment method that enables completely safe reuse of greywater.

CRediT authorship contribution statement

Antonio Faggiano: Writing – original draft, Formal analysis, Methodology. **Maria Ricciardi:** Writing – review & editing, Methodology. **Oriana Motta:** Conceptualization, Supervision, Writing – review & editing. **Antonino Fiorentino:** Conceptualization, Supervision, Writing – review & editing, Project administration. **Antonio Proto:** Conceptualization, Supervision, Funding acquisition, Writing – review & editing.

Declaration of competing interest

The authors declare that they have no known competing financial interests or personal relationships that could have appeared to influence the work reported in this paper.

Data availability

Data will be made available on request.

Acknowledgments

This work was financially supported by “National Interuniversity Consortium of Material Science and Technology” (INSTM). Authors thank INSTM also for the administrative management. Authors thank Giulia Limone for technical assistance.

Appendix A. Supplementary data

Supplementary data to this article can be found online at https://doi.org/10.1016/j.jclepro.2023.137792.

References

Abeledo-Lameiro, M., Polo-López, M., Ares-Mazás, E., Gómez-Couso, H., 2019. Inactivation of the waterborne pathogen Cryptosporidium parvum by photo-Fenton process under natural solar conditions. Appl. Catal. B Environ. 253 https://doi.org/10.1016/j.apcatb.2019.04.049.

Agenda 2030 [WWW Document], n.d. . ONU Italia. URL. https://unric.org/it/agenda-2030/. (Accessed 28 February 2023).

Albalawneh, A., Chang, T.-K., 2015. Review of the greywater and proposed greywater recycling scheme for agricultural irrigation reuses. Int. J. Regul. Govern. 3, 16–35. https://doi.org/10.29121/granthaalayah.v3.i12.2015.2882.

APHA, 1998. Standard Methods for the Examination of Water and Waste Water.

Arellano, M., Pazos, M., Sanromán, M.Á., 2019. Sulfate radicals-based technology as a promising strategy for wastewater. Water 11, 1695. https://doi.org/10.3390/w11081695.

Blanky, M., Rodríguez-Martínez, S., Halpern, M., Friedler, E., 2015. Legionella pneumophila: from potable water to treated greywater; quantification and removal during treatment. Sci. Total Environ. 533, 557–565. https://doi.org/10.1016/j.scitotenv.2015.06.121.

Boyjoo, Y., Pareek, V.K., Ang, M., 2013. A review of greywater characteristics and treatment processes. Water Sci. Technol. 67, 1403–1424. https://doi.org/10.2166/wst.2013.675.

Chin, W.H., Roddick, F.A., Harris, J.L., 2009. Greywater treatment by UVC/H2O2. Water Res. 43, 3940–3947. https://doi.org/10.1016/j.watres.2009.06.050.

Cibati, A., Gonzalez-Olmos, R., Rodriguez-Mozaz, S., Buttiglieri, G., 2022. Unravelling the performance of UV/H2O2 on the removal of pharmaceuticals in real industrial, hospital, grey and urban wastewaters. Chemosphere 290, 133315. https://doi.org/10.1016/j.chemosphere.2021.133315.

Conte, L.O., Farias, J., Albizzati, E.D., Alfano, O.M., 2012. Photo-fenton degradation of the herbicide 2,4-dichlorophenoxyacetic acid in laboratory and solar pilot-plant reactors. Ind. Eng. Chem. Res. 51, 4181–4191. https://doi.org/10.1021/ie2023228.

de Simone Souza, H.H., Falqui, L., Xuereb, R., Mamo, J., Abela, S., Grech, M., Refalo, P., 2023. Environmental assessment of a single-family photocatalytic greywater treatment system based on the design and operating conditions. Sustain. Prod. Consum. 35, 483–494. https://doi.org/10.1016/j.spc.2022.12.001.

Decreto Legislativo 152/06 "Norme in materia ambientale," 2006, dos Santos, P.R., de Oliveira Dourados, M.E., Sirés, I., Brillas, E., Cavalcante, R.P., Cavalheri, P.S., Paulo, P.L., Guelfi, D.R.V., Oliveira, S.C. de, Gozzi, F., Machulek Junior, A., 2023. Greywater treatment by anodic oxidation, photoelectro-Fenton and solar photoelectro-Fenton processes: influence of relevant parameters and toxicity evolution. Process Saf. Environ. Protect. 169, 879–895. https://doi.org/10.1016/j.psep.2022.11.058.

Elmitwalli, T.A., Otterpohl, R., 2007. Anaerobic biodegradability and treatment of grey water in upflow anaerobic sludge blanket (UASB) reactor. Water Res. 41, 1379–1387. https://doi.org/10.1016/j.watres.2006.12.016.

Faggiano, A., De Carluccio, M., Fiorentino, A., Ricciardi, M., Cucciniello, R., Proto, A., Rizzo, L., 2023. Photo-Fenton like process as polishing step of biologically co-treated olive mill wastewater for phenols removal. Sep. Purif. Technol. 305, 122525 https://doi.org/10.1016/j.seppur.2022.122525.

Faggiano, A., Ricciardi, M., Fiorentino, A., Cucciniello, R., Motta, O., Rizzo, L., Proto, A., 2022. Combination of foam fractionation and photo-Fenton like processes for greywater treatment. Sep. Purif. Technol. 293, 121114 https://doi.org/10.1016/j.seppur.2022.121114.

Filali, H., Barsan, N., Souguir, D., Nedeff, V., Tomozei, C., Hachicha, M., 2022. Greywater as an alternative solution for a sustainable management of water resources—a review. Sustainability 14, 665. https://doi.org/10.3390/su14020665.

Fiorentino, A., Esteban, B., Garrido-Cardenas, J.A., Kowalska, K., Rizzo, L., Aguera, A., Pérez, J.A.S., 2019. Effect of solar photo-Fenton process in raceway pond reactors at neutral pH on antibiotic resistance determinants in secondary treated urban wastewater. J. Hazard Mater. 378, 120737 https://doi.org/10.1016/j.jhazmat.2019.06.014.

Fiorentino, A., Ferro, G., Alferez, M.C., Polo-López, M.I., Fernández-Ibañez, P., Rizzo, L., 2015. Inactivation and regrowth of multidrug resistant bacteria in urban wastewater after disinfection by solar-driven and chlorination processes. J. Photochem. Photobiol. B Biol. 148, 43–50. https://doi.org/10.1016/j.jphotobiol.2015.03.029.

Fiorentino, A., Lofrano, G., Cucciniello, R., Carotenuto, M., Motta, O., Proto, A., Rizzo, L., 2021. Disinfection of roof harvested rainwater inoculated with E. coli and Enterococcus and post-treatment bacterial regrowth: conventional vs solar driven advanced oxidation processes. Sci. Total Environ. 801, 149763 https://doi.org/10.1016/j.scitotenv.2021.149763.

Fiorentino, A., Rizzo, L., Guilloteau, H., Bellanger, X., Merlin, C., 2017. Comparing TiO2 photocatalysis and UV-C radiation for inactivation and mutant formation of Salmonella typhimurium TA102. Environ. Sci. Pollut. Res. 24, 1871–1879. https://doi.org/10.1007/s11356-016-7981-6.

Fiorentino, A., Soriano-Molina, P., Abeledo-Lameiro, M.J., de la Obra, I., Proto, A., Polo-López, M.I., Pérez, J.A.S., Rizzo, L., 2022. Neutral (Fe3+-NTA) and acidic (Fe2+) pH solar photo-Fenton vs chlorination: effective urban wastewater disinfection does not mean control of antibiotic resistance. J. Environ. Chem. Eng. 10, 108777 https://doi.org/10.1016/j.jece.2022.108777.

Ghaitidak, D.M., Yadav, K.D., 2013. Characteristics and treatment of greywater—a review. Environ. Sci. Pollut. Res. 20, 2795–2809. https://doi.org/10.1007/s11356-013-1533-0.

Ghanbari, F., Moradi, M., 2017. Application of peroxymonosulfate and its activation methods for degradation of environmental organic pollutants: review. Chem. Eng. J. 310, 41–62. https://doi.org/10.1016/j.cej.2016.10.064.

Giménez, B.N., Conte, L.O., Audino, F., Schenone, A.V., Graells, M., Alfano, O.M., Pérez-Moya, M., 2023. Kinetic model of photo-Fenton degradation of paracetamol in an annular reactor: main reaction intermediates and cytotoxicity studies. Catalysis Today, Solar chemistry & photocatalysis: environmental applications – SPEA11 413–415, 113958 https://doi.org/10.1016/j.cattod.2022.11.019.

Gómez-Monsalve, M., Domínguez, I.C., Yan, X., Ward, S., Oviedo-Ocaña, E.R., 2022. Environmental performance of a hybrid rainwater harvesting and greywater reuse system: a case study on a high water consumption household in Colombia. J. Clean. Prod. 345, 131125 https://doi.org/10.1016/j.jclepro.2022.131125.

Gualda-Alonso, E., Soriano-Molina, P., García Sánchez, J.L., Casas López, J.L., Sánchez Pérez, J.A., 2022. Mechanistic modeling of solar photo-Fenton with Fe3+-NTA for microcontaminant removal. Appl. Catal. B Environ. 318, 121795 https://doi.org/10.1016/j.apcatb.2022.121795.

Hardie, A.G., Madubela, N., Clarke, C.E., Lategan, E.L., 2021. Impact of powdered and liquid laundry detergent greywater on soil degradation. J. Hydrol. 595, 126059 https://doi.org/10.1016/j.jhydrol.2021.126059.

Jurado, E., Fernández-Serrano, M., Núñez-Olea, J., Luzón, G., Lechuga, M., 2006. Simplified spectrophotometric method using methylene blue for determining anionic surfactants: applications to the study of primary biodegradation in aerobic screening tests. Chemosphere 65, 278–285. https://doi.org/10.1016/j.chemosphere.2006.02.044.

Kadewa, W.W., Knops, G., Pidou, M., Jeffrey, P., Jefferson, B., Le Corre, K.S., 2020. What is the impact of personal care products selection on greywater characteristics and reuse? Sci. Total Environ. 749, 141413 https://doi.org/10.1016/j.scitotenv.2020.141413.

Kamaya, M., Kaneko, Y., Nagashima, K., 1999. Simple method for spectrophotometric determination of cationic surfactants without liquid–liquid extraction. Anal. Chim. Acta 384, 215–218. https://doi.org/10.1016/S0003-2670(98)00854-X.

Karim, A.V., Jiao, Y., Zhou, M., Nidheesh, P.V., 2021. Iron-based persulfate activation process for environmental decontamination in water and soil. Chemosphere 265, 129057. https://doi.org/10.1016/j.chemosphere.2020.129057.

Khanam, K., Patidar, S.K., 2022. Greywater characteristics in developed and developing countries. Mater. Today: Proceedings, International Chemical Engineering Conference 2021 (100 Glorious Years of Chemical Engineering & Technology) 57, 1494–1499. https://doi.org/10.1016/j.matpr.2021.12.022.

Khosravanipour Mostafazadeh, A., Benguit, A.T., Carabin, A., Drogui, P., Brien, E., 2019. Development of combined membrane filtration, electrochemical technologies, and adsorption processes for treatment and reuse of laundry wastewater and removal of nonylphenol ethoxylates as surfactants. J. Water Process Eng. 28, 277–292. https://doi.org/10.1016/j.jwpe.2019.02.014.

Kummu, M., Guillaume, J.H.A., de Moel, H., Eisner, S., Flörke, M., Porkka, M., Siebert, S., Veldkamp, T.I.E., Ward, P.J., 2016. The world's road to water scarcity: shortage and stress in the 20th century and pathways towards sustainability. Sci. Rep. 6, 38495 https://doi.org/10.1038/srep38495.

Kusic, H., Peternel, I., Ukic, S., Koprivanac, N., Bolanca, T., Papic, S., Bozic, A.L., 2011. Modeling of iron activated persulfate oxidation treating reactive azo dye in water matrix. Chem. Eng. J. 172, 109–121. https://doi.org/10.1016/j.cej.2011.05.076.

Lechuga, M., Fernández-Serrano, M., Jurado, E., Núñez-Olea, J., Ríos, F., 2016. Acute toxicity of anionic and non-ionic surfactants to aquatic organisms. Ecotoxicol. Environ. Saf. 125, 1–8. https://doi.org/10.1016/j.ecoenv.2015.11.027.

Li, F., Wichmann, K., Otterpohl, R., 2009. Review of the technological approaches for grey water treatment and reuses. Sci. Total Environ. 407, 3439–3449. https://doi.org/10.1016/j.scitotenv.2009.02.004.

Li, J., Tao, T., Li, X., Zuo, J., Li, T., Lu, J., Li, S., Chen, L., Xia, C., Liu, Y., Wang, Y., 2009. A spectrophotometric method for determination of chemical oxygen demand using home-made reagents. Desalination 239, 139–145. https://doi.org/10.1016/j.desal.2008.03.014.

Liang, C., Huang, C.-F., Mohanty, N., Kurakalva, R.M., 2008. A rapid spectrophotometric determination of persulfate anion in ISCO. Chemosphere 73, 1540–1543. https://doi.org/10.1016/j.chemosphere.2008.08.043.

Lin, X., Ma, Y., Wang, Y., Wan, J., Guan, Z., 2015. Lithium iron phosphate (LiFePO4) as an effective activator for degradation of organic dyes in water in the presence of persulfate. RSC Adv. 5, 94694–94701. https://doi.org/10.1039/C5RA19697C.

Liu, C.S., Shih, K., Sun, C.X., Wang, F., 2012. Oxidative degradation of propachlor by ferrous and copper ion activated persulfate. Sci. Total Environ. 416, 507–512. https://doi.org/10.1016/j.scitotenv.2011.12.004.

Maimon, A., Tal, A., Friedler, E., Gross, A., 2010. Safe on-site reuse of greywater for irrigation - a critical review of current guidelines. Environ. Sci. Technol. 44, 3213–3220. https://doi.org/10.1021/es902646g.

Mekonnen, M.M., Hoekstra, A.Y., 2016. Four billion people facing severe water scarcity. Sci. Adv. 2, e1500323 https://doi.org/10.1126/sciadv.1500323.

Noah, M., 2002. Graywater use still a gray area. J. Environ. Health 64, 22–25.

O'Dowd, K., Pillai, S.C., 2020. Photo-Fenton disinfection at near neutral pH: process, parameter optimization and recent advances. J. Environ. Chem. Eng. 8, 104063 https://doi.org/10.1016/j.jece.2020.104063.

Palmer, M., Hatley, H., 2018. The role of surfactants in wastewater treatment: impact, removal and future techniques: a critical review. Water Res. 147, 60–72. https://doi.org/10.1016/j.watres.2018.09.039.

Pesqueira, J.F.J.R., Pereira, M.F.R., Silva, A.M.T., 2021. A life cycle assessment of solar-based treatments (H2O2, TiO2 photocatalysis, circumneutral photo-Fenton) for the

removal of organic micropollutants. Sci. Total Environ. 761, 143258 https://doi.org/10.1016/j.scitotenv.2020.143258.
Pidou, M., Memon, F.A., Stephenson, T., Jefferson, B., Jeffrey, P., 2007. Greywater recycling: treatment options and applications. Proceedings of the Institution of Civil Engineers - Engineering Sustainability 160, 119–131. https://doi.org/10.1680/ensu.2007.160.3.119.
Pignatello, J.J., Oliveros, E., MacKay, A., 2006. Advanced oxidation processes for organic contaminant destruction based on the fenton reaction and related chemistry. Crit. Rev. Environ. Sci. Technol. 36, 1–84. https://doi.org/10.1080/10643380500326564.
Pontes, R.F.F., Moraes, J.E.F., Machulek, A., Pinto, J.M., 2010. A mechanistic kinetic model for phenol degradation by the Fenton process. J. Hazard Mater. 176, 402–413. https://doi.org/10.1016/j.jhazmat.2009.11.044.
Ribeiro, J.P., Marques, C.C., Portugal, I., Nunes, M.I., 2020. Fenton processes for AOX removal from a kraft pulp bleaching industrial wastewater: optimisation of operating conditions and cost assessment. J. Environ. Chem. Eng. 8, 104032 https://doi.org/10.1016/j.jece.2020.104032.
Sakai, T., Ohno, N., Kamoto, T., Sasaki, H., 1992. Formation of ternary ion associates using diprotic acid dyes and its application to determination of cationic surfactants. Mikrochim. Acta 106, 45–55. https://doi.org/10.1007/BF01242698.
Schoen, M.E., Jahne, M.A., Garland, J., Ramirez, L., Lopatkin, A.J., Hamilton, K.A., 2021. Quantitative microbial risk assessment of antimicrobial resistant and susceptible Staphylococcus aureus in reclaimed wastewaters. Environ. Sci. Technol. 55, 15246–15255. https://doi.org/10.1021/acs.est.1c04038.
Shaikh, I.N., Ahammed, M.M., 2020. Quantity and quality characteristics of greywater: a review. J. Environ. Manag. 261, 110266 https://doi.org/10.1016/j.jenvman.2020.110266.
Shoushtarian, F., Negahban-Azar, M., 2020. Worldwide regulations and guidelines for agricultural water reuse: a critical review. Water 12, 971. https://doi.org/10.3390/w12040971.
Silva, J.R.M., de Oliveira Celeri, M., Borges, A.C., Fernandes, R.B.A., 2023. Greywater as a water resource in agriculture: the acceptance and perception from Brazilian agricultural technicians. Agric. Water Manag. 280, 108227 https://doi.org/10.1016/j.agwat.2023.108227.
Simunovic, M., Kusic, H., Koprivanac, N., Bozic, A.L., 2011. Treatment of simulated industrial wastewater by photo-Fenton process: Part II. The development of mechanistic model. Chem. Eng. J. 173, 280–289. https://doi.org/10.1016/j.cej.2010.09.030.
Soriano-Molina, P., Miralles-Cuevas, S., Oller, I., García Sánchez, J.L., Sánchez Pérez, J. A., 2021. Contribution of temperature and photon absorption on solar photo-Fenton mediated by Fe3+-NTA for CEC removal in municipal wastewater. Appl. Catal. B Environ. 294, 120251 https://doi.org/10.1016/j.apcatb.2021.120251.
Šostar-Turk, S., Petrinić, I., Simonič, M., 2005. Laundry wastewater treatment using coagulation and membrane filtration. Resour. Conserv. Recycl. 44, 185–196. https://doi.org/10.1016/j.resconrec.2004.11.002.
Spychała, M., Nieć, J., Zawadzki, P., Matz, R., Nguyen, T.H., 2019. Removal of volatile solids from greywater using sand filters. Appl. Sci. 9, 770. https://doi.org/10.3390/app9040770.
Talinli, I., Anderson, G.K., 1992. Interference of hydrogen peroxide on the standard cod test. Water Res. 26, 107–110. https://doi.org/10.1016/0043-1354(92)90118-N.
Teodoro, A., Boncz, M.Á., Júnior, A.M., Paulo, P.L., 2014. Disinfection of greywater pre-treated by constructed wetlands using photo-Fenton: influence of pH on the decay of Pseudomonas aeruginosa. J. Environ. Chem. Eng. 2, 958–962. https://doi.org/10.1016/j.jece.2014.03.013.
Teodoro, A., Júnior, A.M., Boncz, M.Á., Paulo, P.L., 2018. Alternative use of Pseudomonas aeruginosa as indicator for greywater disinfection. Water Sci. Technol. 78, 1361–1369. https://doi.org/10.2166/wst.2018.408.
Tôei, K., Motomizu, S., Umano, T., 1982. Extractive spectrophotometric determination of non-ionic surfactants in water. Talanta 29, 103–106. https://doi.org/10.1016/0039-9140(82)80028-3.
Tsoumachidou, S., Velegraki, T., Antoniadis, A., Poulios, I., 2017. Greywater as a sustainable water source: a photocatalytic treatment technology under artificial and solar illumination. J. Environ. Manag. 195, 232–241. https://doi.org/10.1016/j.jenvman.2016.08.025.
Wagdy, A.H., El-Hazek, A.N., Hassanain, A.M., 2022. Assessment of a fenton reaction in treating greywater for reuse in irrigation. Engineering Research Journal - Faculty of Engineering (Shoubra) 51, 141–148. https://doi.org/10.21608/erjsh.2022.151400.1062.
Ying, G.-G., 2006. Fate, behavior and effects of surfactants and their degradation products in the environment. Environ. Int. 32, 417–431. https://doi.org/10.1016/j.envint.2005.07.004.
Zapata, A., Velegraki, T., Sánchez Pérez, J.A., Mantzavinos, D., Maldonado, M., Malato, S., 2009. Solar photo-Fenton treatment of pesticides in water: effect of iron concentration on degradation and assessment of ecotoxicity and biodegradability. Appl. Catal. B Environ. 88, 448–454. https://doi.org/10.1016/j.apcatb.2008.10.024.
Zhang, H., Wang, Z., Liu, C., Guo, Y., Shan, N., Meng, C., Sun, L., 2014. Removal of COD from landfill leachate by an electro/Fe2+/peroxydisulfate process. Chem. Eng. J. 250, 76–82. https://doi.org/10.1016/j.cej.2014.03.114.
Zhou, L., 2017. Sulfate-radical Induced Removal of Organic Micro-pollutants from Aqueous Solution- Influence of Natural Water Constituents (Phdthesis). Université de Lyon.
Ziemba, C., Larivé, O., Reynaert, E., Morgenroth, E., 2018. Chemical composition, nutrient-balancing and biological treatment of hand washing greywater. Water Res. 144, 752–762. https://doi.org/10.1016/j.watres.2018.07.005.